Active galactic nuclei (AGNs): a brief observational tour

Yongquan Xue (薛永泉)

Department of Astronomy
University of Science and Technology of China
http://staff.ustc.edu.cn/~xuey

Summary of lectures

- Early history, AGN ABCs, finding AGNs, AGN terminology and unification
- Dissecting AGNs (I): black hole, accretion disk, broad line region
- Dissecting AGNs (II): torus, narrow line region, stars and starburst regions, jets
- Focused lecture: Lifting the veil of deeply buried supermassive black holes in the Universe

Summary of lectures

- Early history, AGN ABCs, finding AGNs, AGN terminology and unification
- Dissecting AGNs (I): black hole, accretion disk, broad line region
- Dissecting AGNs (II): torus, narrow line region, stars and starburst regions, jets
- **Focused lecture: Lifting the veil of deeply buried supermassive black holes in the Universe**

Lifting the Veil of Deeply Buried Supermassive Black Holes in the Universe

Outline

- Highly-obscured/Compton-thick AGNs
- Recent efforts in searching for these AGNs in the CDF-S
- Summary
- Prospects

Outline

- Highly-obscured/Compton-thick AGNs
- Recent efforts in searching for these AGNs in the CDF-S
- Summary
- Prospects

Orientation-based unified models for AGNs

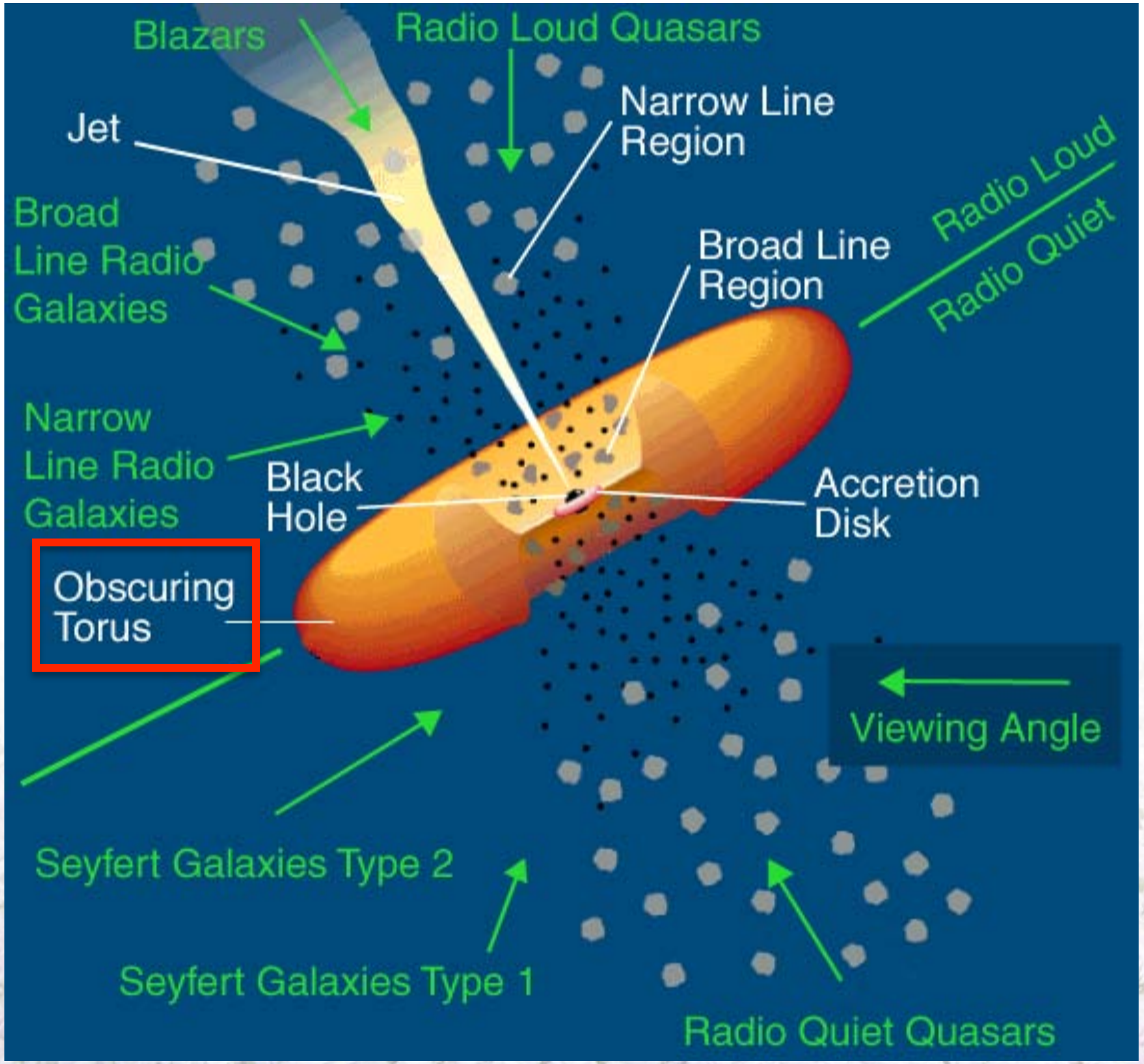

(NASA)

- X-ray unobscured: <1E21 cm^(-2)
- Obscured Compton-thin: 1E21 – 1E24
- Compton-thick (CT): >1e24 (mildly/heavily)

Obscuring torus

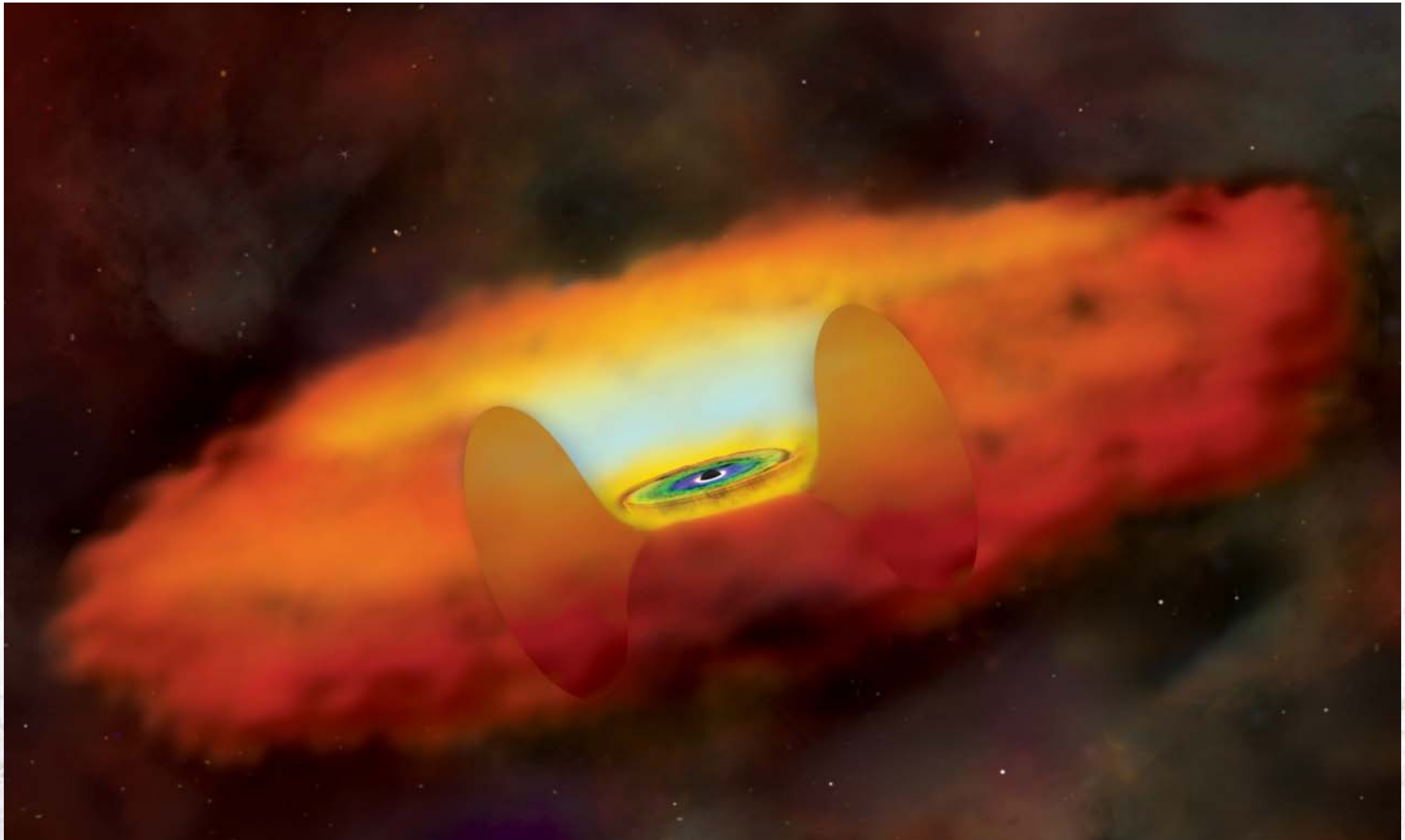

Obscuring torus

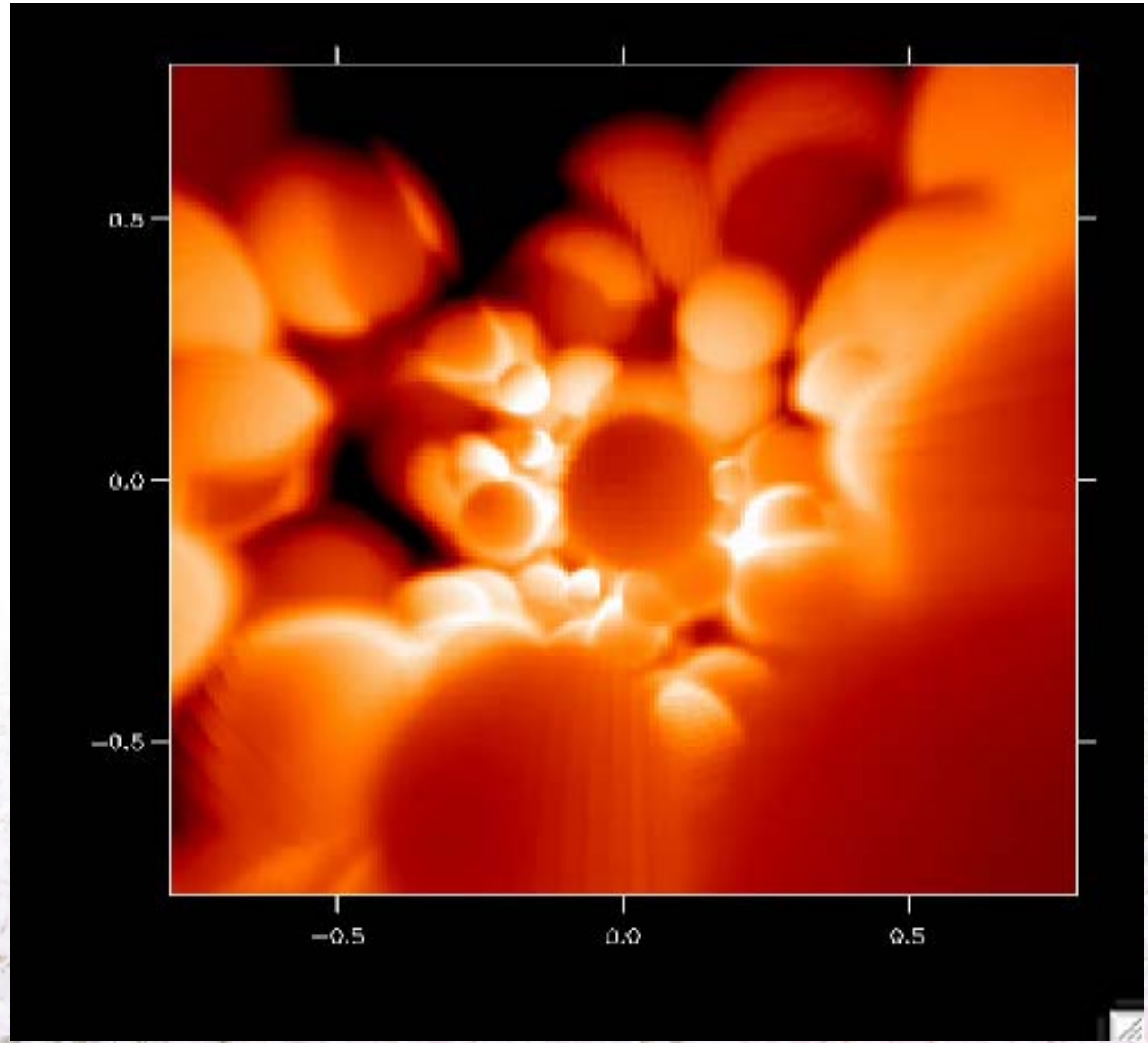

(Credit: C. P. Dullemond)

Highly-obscured AGNs/CT-AGNs

$$\tau \sim n\sigma l \sim N_H \sigma_T \sim 1, \text{ so } N_H \sim 10^{24}$$

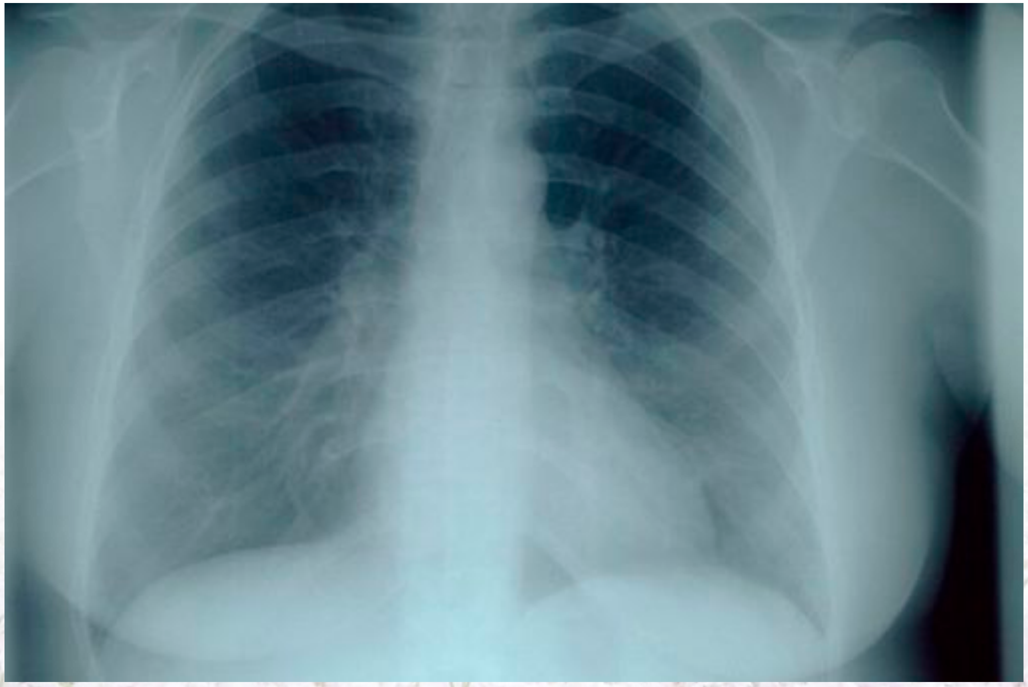

- Highly-obscured AGNs: >3e23 cm^(-2)

Why do we care about CT-AGNs?

- Observational evidence suggesting that a large fraction of local AGNs are obscured by CT gas (e.g., Maiolino+98, Risaliti+99, Matt+00)

Why do we care about CT-AGNs?

- Observational evidence suggesting that a large fraction of local AGNs are obscured by CT gas (e.g., Maiolino+98, Risaliti+99, Matt+00)

- Required by AGN synthesis models for X-ray background (e.g., Gilli+07); number density being the same order as that of moderately obscured AGNs

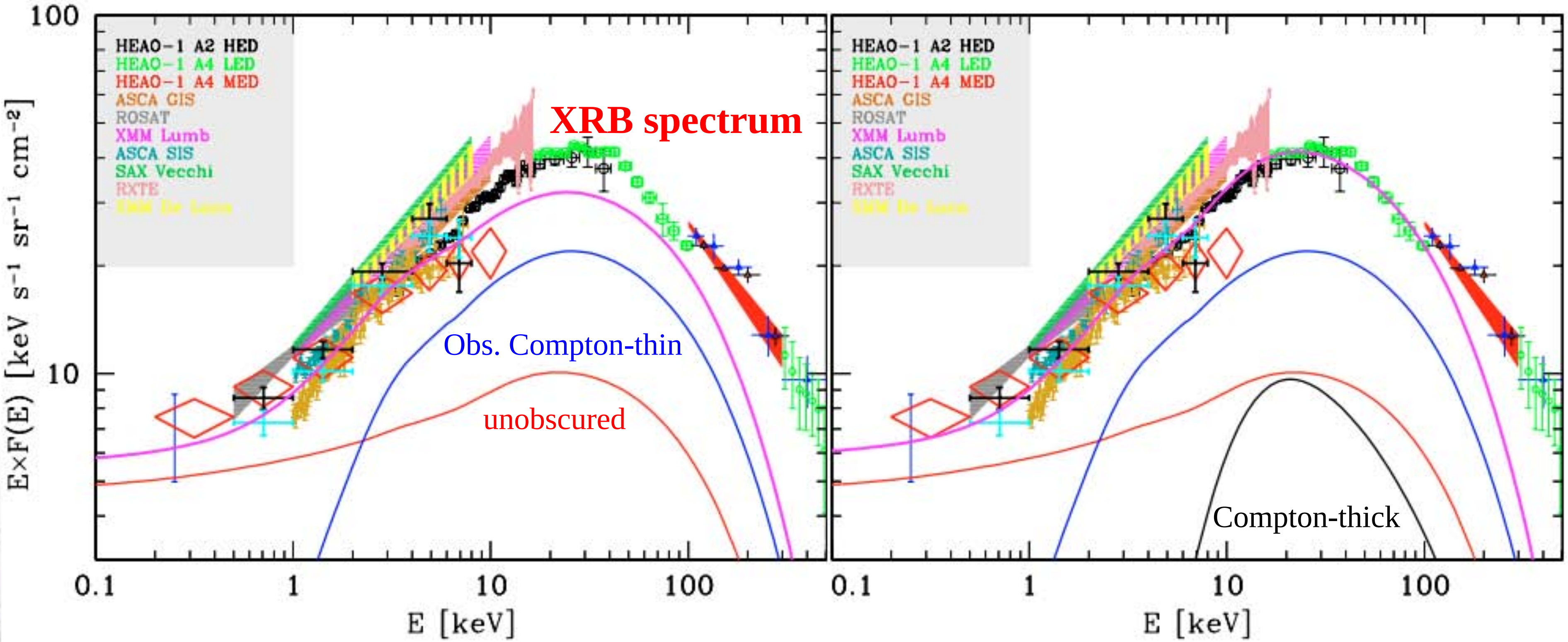

(Gilli, Comastri, & Hasinger 2007)

Why do we care about CT-AGNs?

- Observational evidence suggesting that a large fraction of local AGNs are obscured by CT gas (e.g., Maiolino+98, Risaliti+99, Matt+00)

- Required by AGN synthesis models for X-ray background (e.g., Gilli+07); number density being the same order as that of moderately obscured AGNs

- Distant heavily obscured AGNs represent a crucial black-hole growth phase

Most of them escape even from the deepest X-ray surveys!
Don’t even know their space density and cosmological evolution!

Signatures of Compton-thick emission

- Presence of a strong iron K-alpha line complex at ~6.4 keV

Typical AGN X-ray spectra (*N_H* effects)

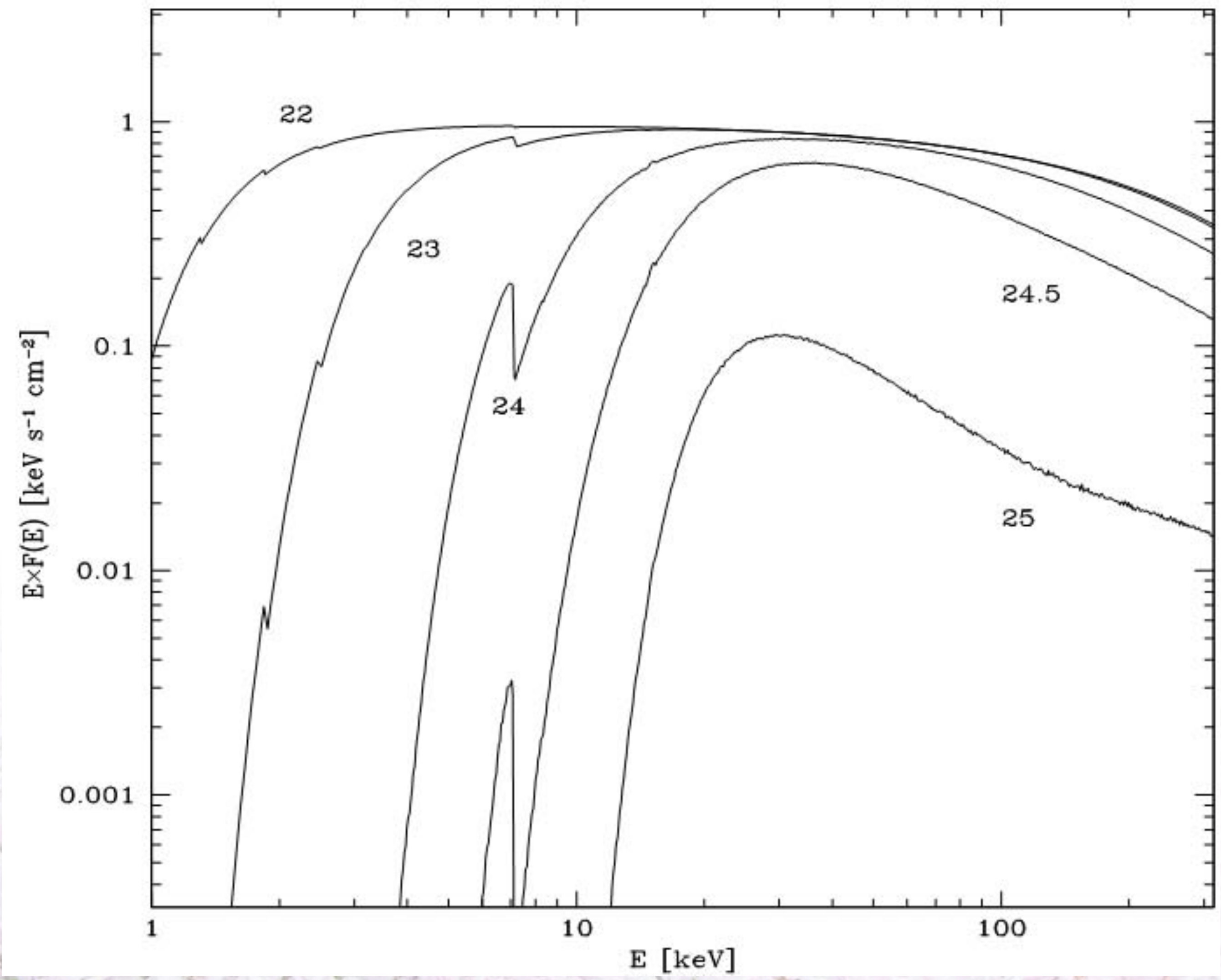

(Comastri 2004)

Signatures of Compton-thick emission

- Presence of a strong iron K-alpha line complex at 6.4-7 keV

- Characteristic reflection spectrum

Spectrum reflected by Compton-thick gas

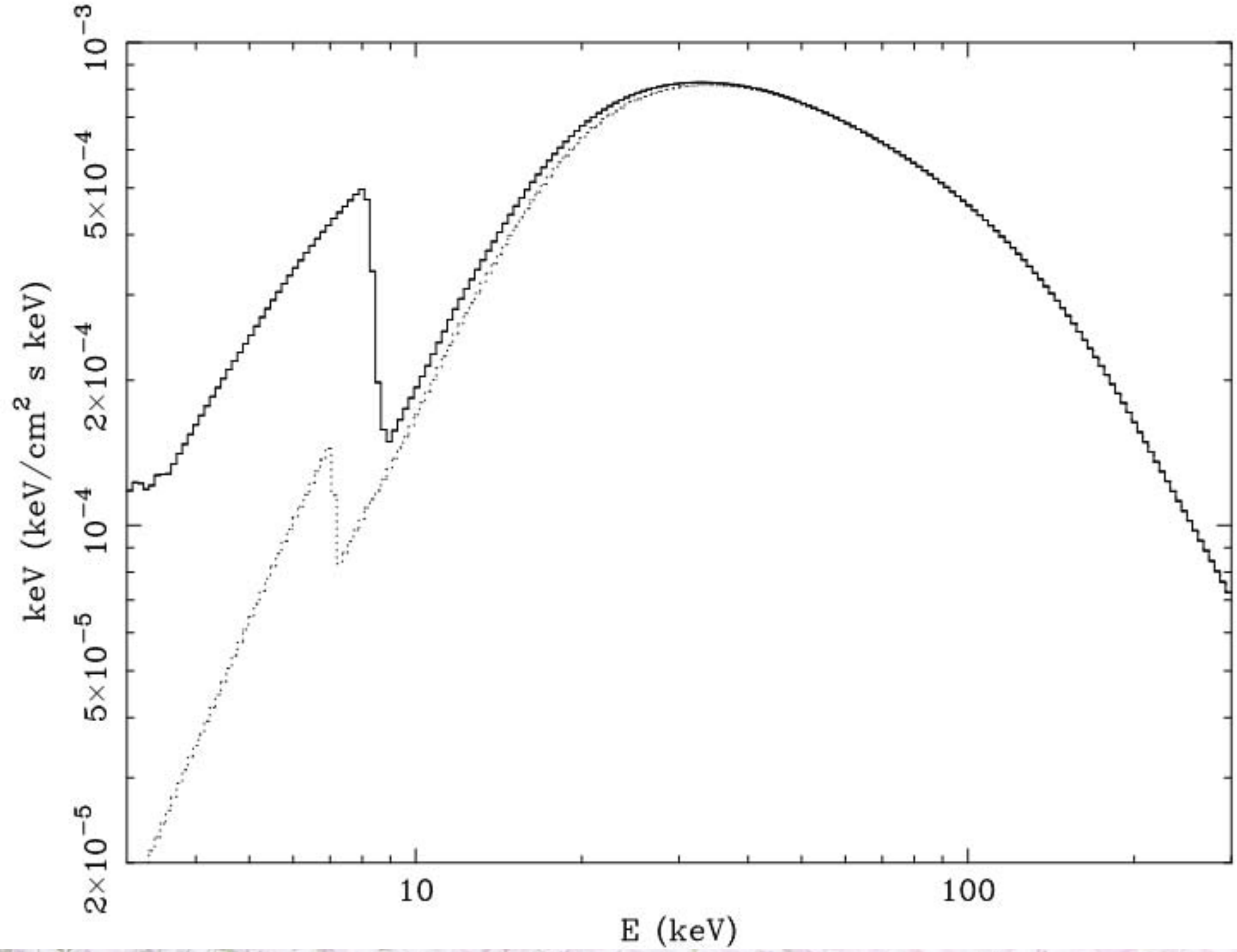

(Comastri 2004)

Signatures of Compton-thick emission

- Presence of a strong iron K-alpha line complex at 6.4-7 keV
- Characteristic reflection spectrum
- IR-excess emission

Home in on the waste heat – AGN heated dust

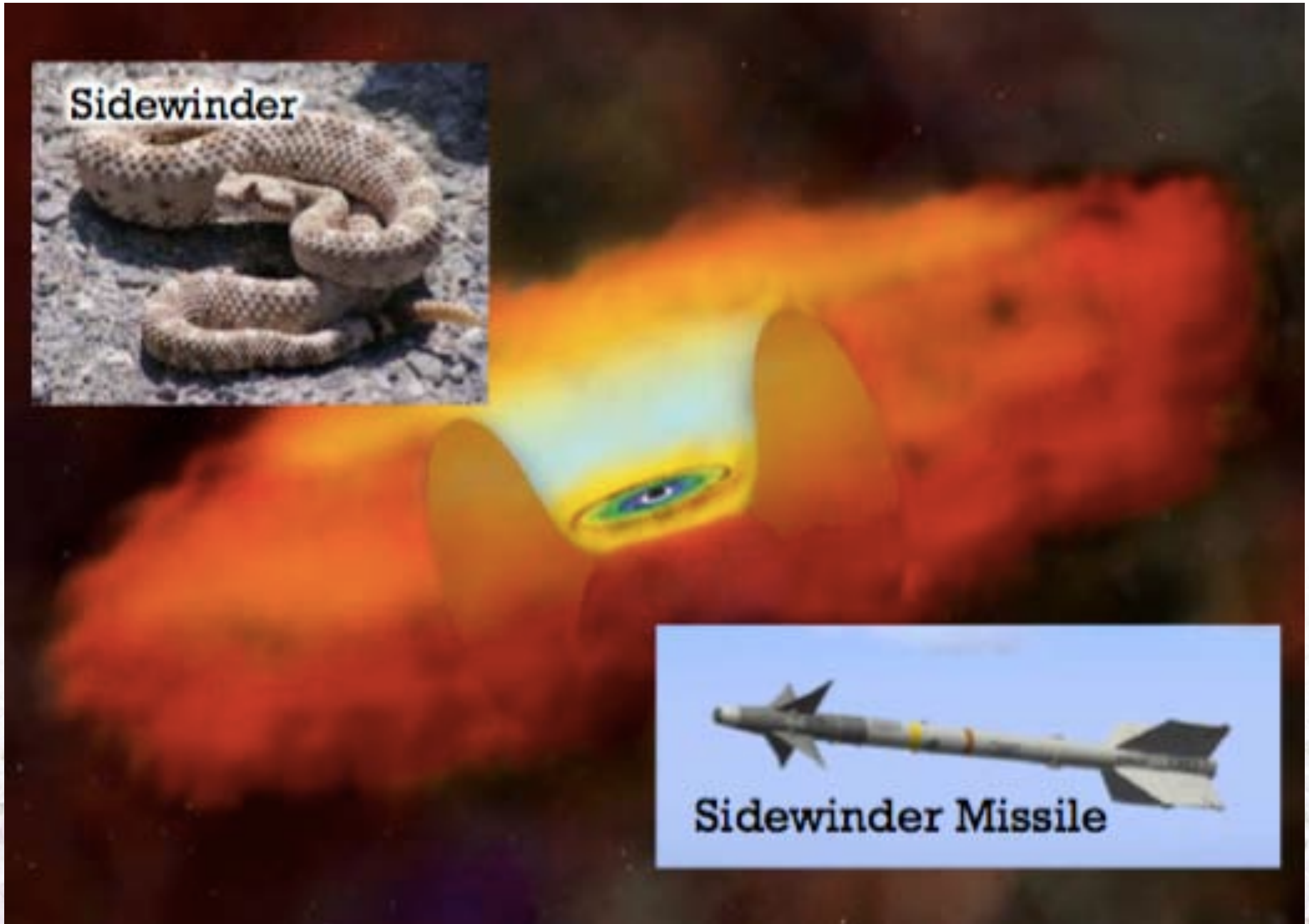

中国科学技术大学
University of Science and Technology of China

Signatures of Compton-thick emission

- Presence of a strong iron K-alpha line complex at 6.4-7 keV
- Characteristic reflection spectrum
- IR-excess emission
- Stacking analysis

Stacking: A Romantic Example

3 / 100 second exposure

1 / 1000 second exposure

Stacked image →

30 candles with 1/1000 sec exposure = 3/100 sec

Outline

- Highly-obscured/Compton-thick AGNs
- Recent efforts in searching for these AGNs in the CDF-S
- Summary
- Prospects

Utility of deep extragalactic X-ray surveys

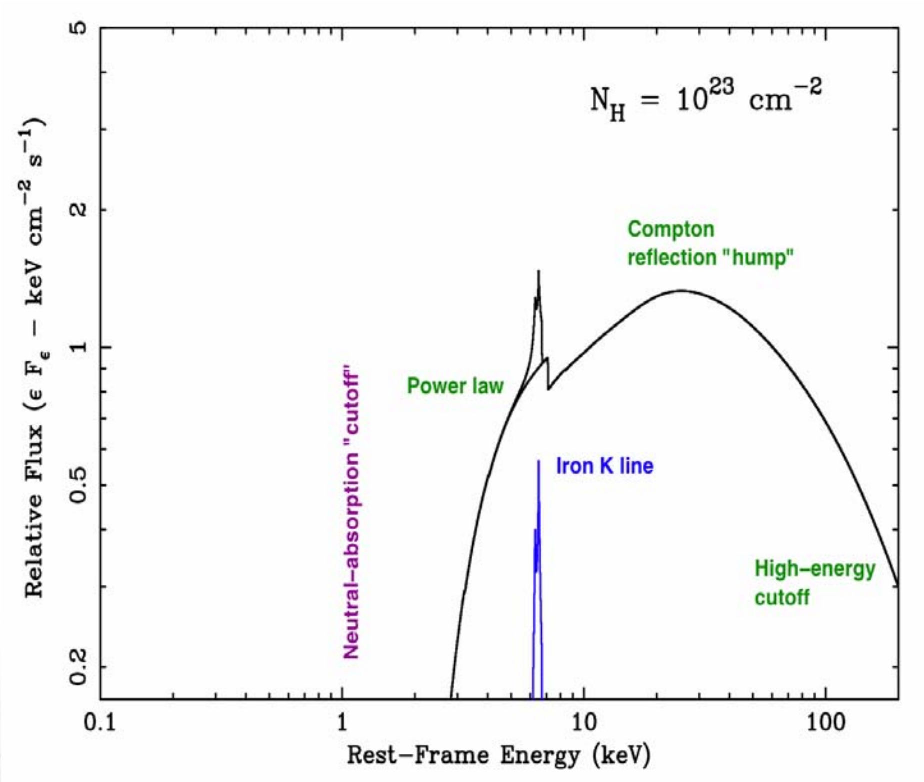

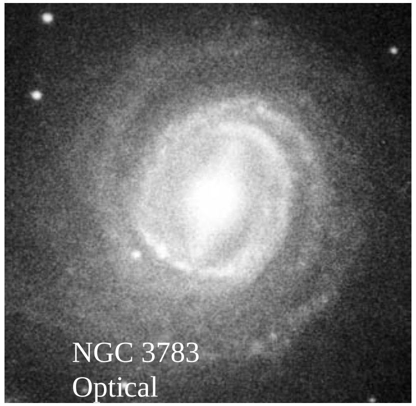

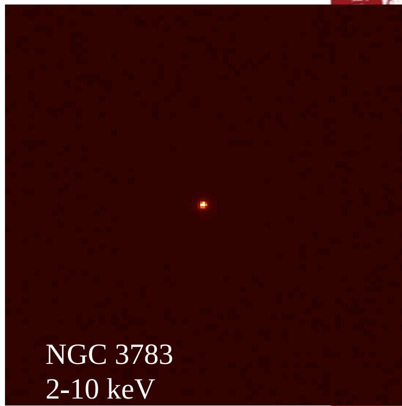

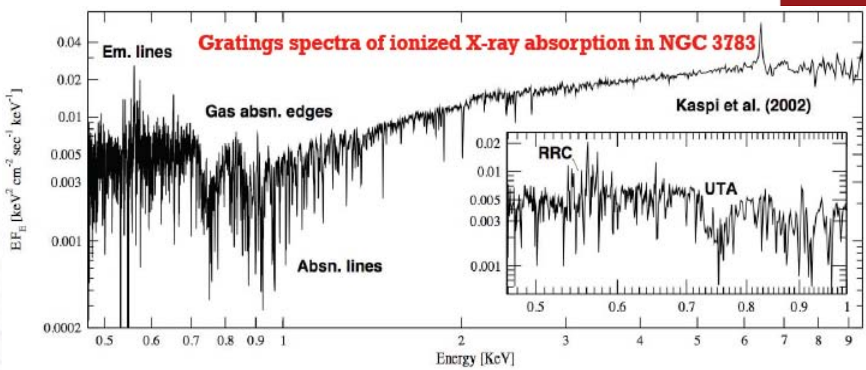

- X-ray: nearly universal signature of luminous AGNs
- Reduced absorption bias for majority population
- Minimal dilution by host starlight
- X-ray spectra of AGNs: rich of diagnostics

Chandra and XMM-Newton

- Up to 80-400 times sensitive than previous missions
- Good-to-great positions (0.2-2.5 arcsec)
- Broad bandpass and respectable filed-of-views
- Hundreds-to-thousands of sources for powerful statistical studies
- ***Chandra*** *has better angular resolution, lower background, and largely no source confusion*

X-ray survey discovery space

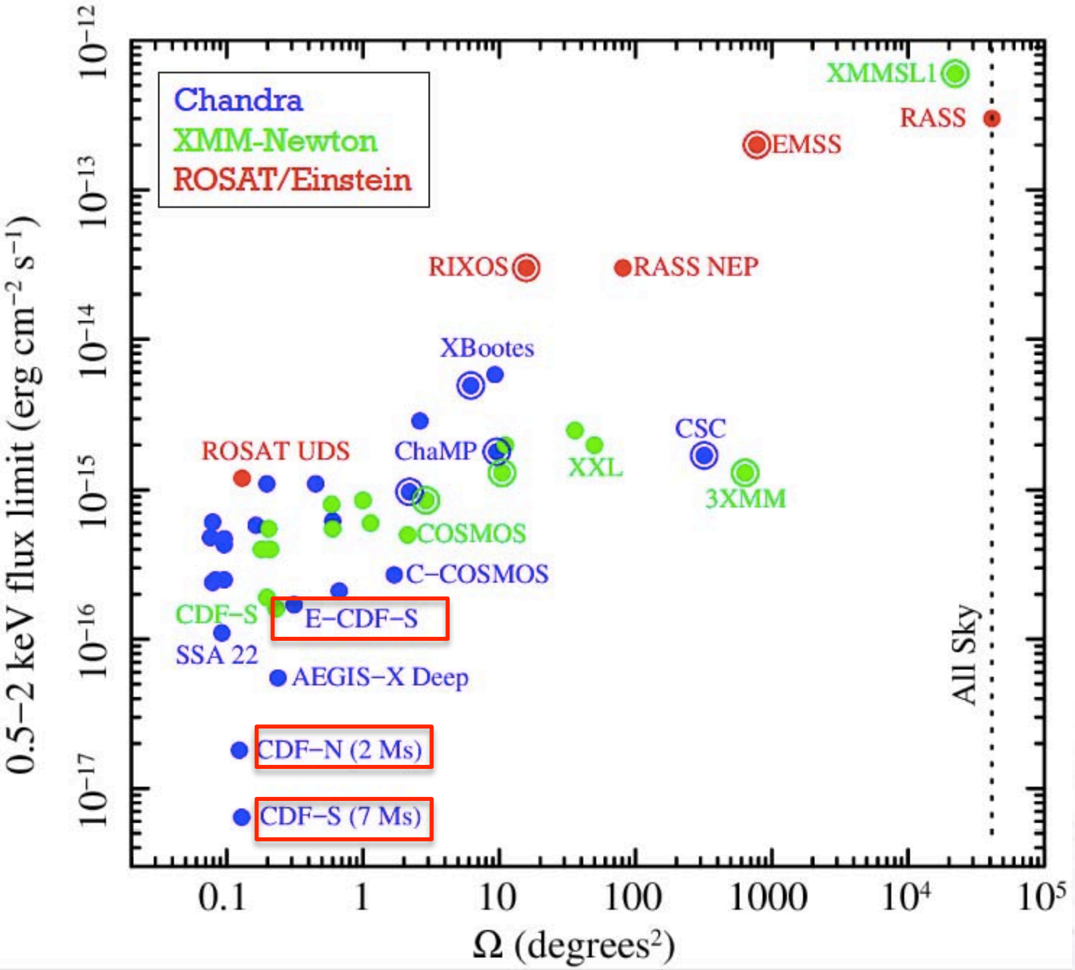

Updated from Brandt & Alexander (2015)

- ~25 major Chandra and XMM-Newton surveys
- Cover most of the practically accesible discovery space
- Provide a comprehensive understanding of X-ray source populations

University of Science and Technology of China 中国科学技术大学

The Chandra Deep Fields (CDFs)

7Ms CDF-S

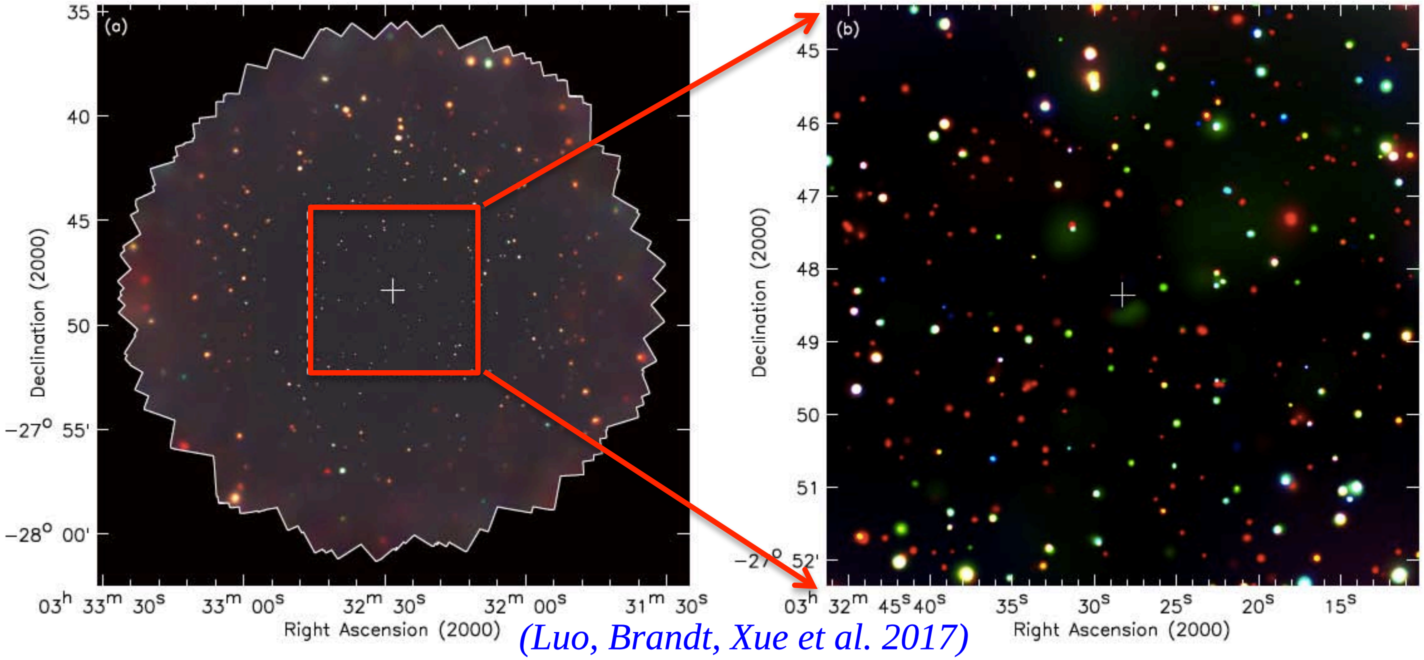

7Ms CDF-S (central)

(Luo, Brandt, Xue et al. 2017)

2Ms CDF-N

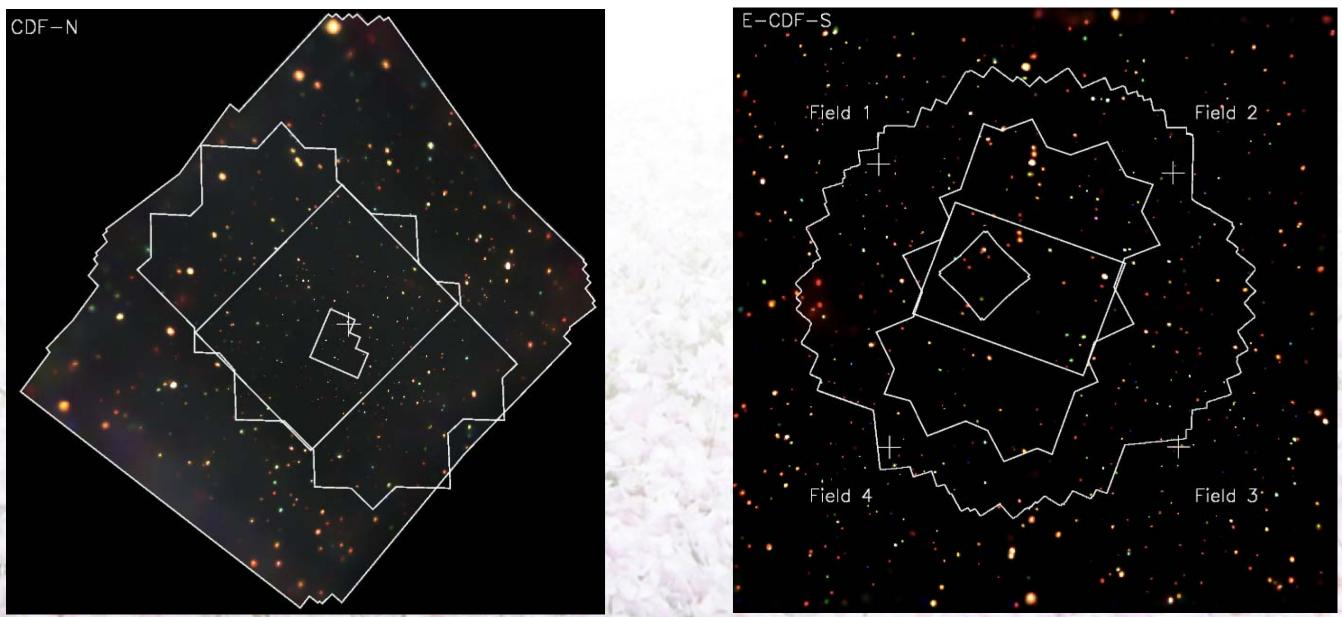

250ks E-CDF-S

(Xue, Luo, Brandt et al. 2016)

中国科学技术大学
University of Science and Technology of China

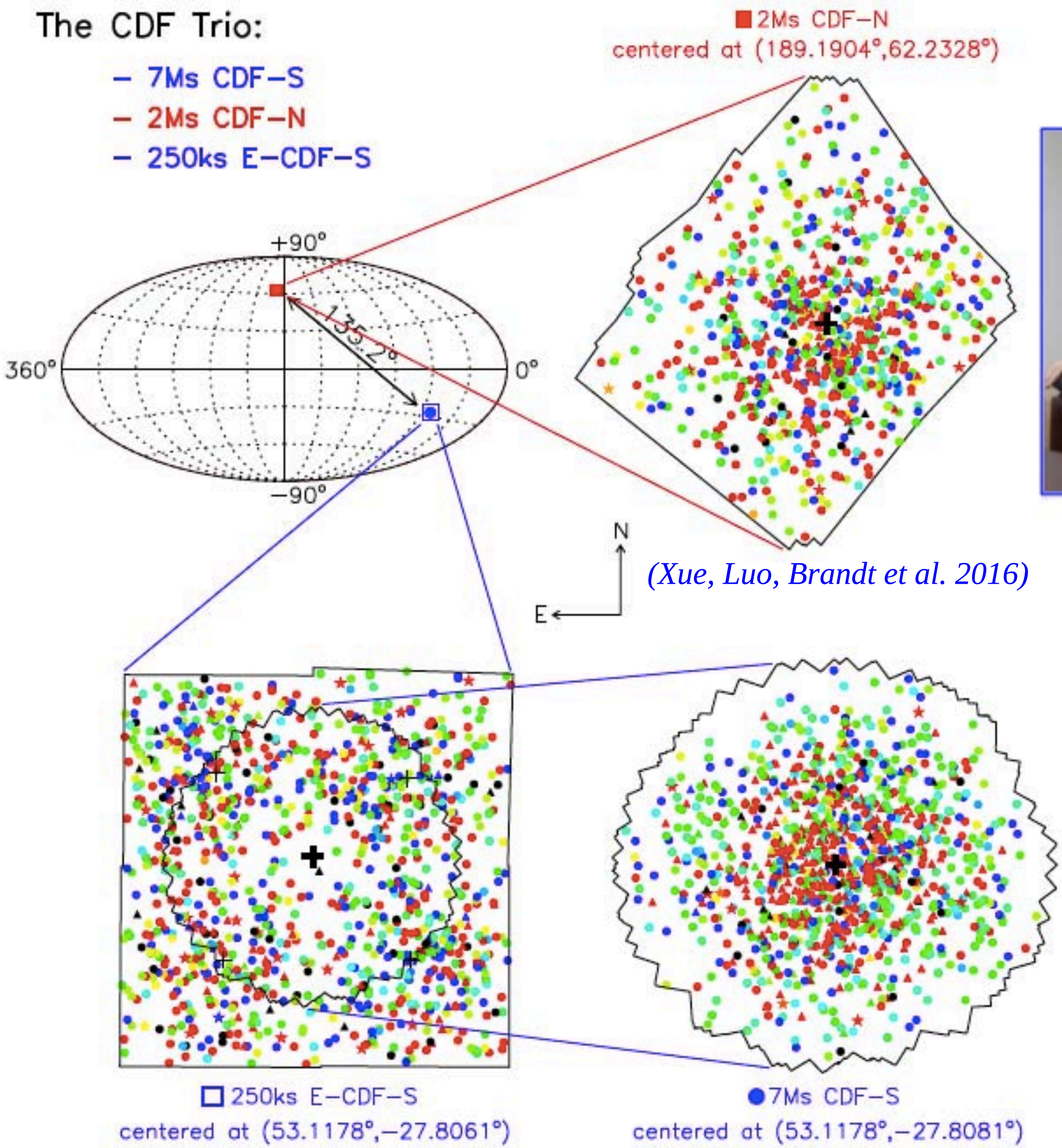

(Xue, Luo, Brandt et al. 2016)

(20161028@USTC)

The 2016 Rossi Prize was awarded to Professor **Niel Brandt** of The Pennsylvania State University, who led the effort to obtain the **deepest Chandra fields**, enabling the most sensitive cosmological X-ray surveys to date. His work traces the accretion history of SMBH and their coevolution with host galaxies across cosmic time.

(Xue, Luo, Brandt et al. 2016) *(Luo, Brandt, Xue et al. 2017)*

Table 1: Properties of the CDFs[a]

	CDF-S	CDF-N	E-CDF-S
Galactic N_H (cm^{-2})	8.8×10^{19}	1.6×10^{20}	8.8×10^{19}
Observational timespan	1999/10 – 2016/03 (16.4 yrs)	1999/11 – 2002/02 (2.3 yrs)	2004/02 – 2004/11 (0.8 yrs)
Total number of observations	102	20	9
Effective exposure (ks)	6727	1896	235/209/240/241[b]
Solid angle covered (arcmin^2)	484.2	447.5	1128.6
Source detection criteria	WAVDETECT at 10^{-5} and $P < 0.007$[c]	WAVDETECT at 10^{-5} and $P < 0.004$	WAVDETECT at 10^{-5} and $P < 0.002$
Number of sources detected	1008	683	1003
FB detected counts	(11.2, 98.9, 56916.2)[d]	(8.1, 66.2, 19748.4)	(3.3, 27.1, 4010.6)
SB detected counts	(6.1, 47.4, 38817.0)	(5.4, 35.0, 14227.3)	(2.2, 18.9, 2802.6)
HB detected counts	(9.2, 94.6, 18137.8)	(7.7, 57.5, 5540.6)	(3.4, 20.4, 1210.8)
1σ X-ray positional uncertainty (")	(0.11, 0.47, 1.28)	(0.10, 0.47, 2.02)	(0.10, 0.63, 1.30)
Logarithm of FB flux (erg cm^{-2} s^{-1})	(−16.76, −15.50, −12.96)	(−16.35, −15.09, −12.70)	(−15.73, −14.79, −12.88)
Logarithm of SB flux (erg cm^{-2} s^{-1})	(−17.11, −16.19, −13.29)	(−16.83, −15.79, −13.07)	(−16.13, −15.27, −13.26)
Logarithm of HB flux (erg cm^{-2} s^{-1})	(−16.46, −15.25, −13.13)	(−16.15, −14.95, −12.95)	(−15.73, −14.70, −13.02)
Faintest sources	1 count per ≈ 10 days	1 count per ≈ 4 days	1 count per ≈ 1 day
Logarithm of $L_{0.5-7\ \mathrm{keV}}$ (erg s^{-1})[e]	(39.01, 42.48, 45.05)	(39.28, 42.94, 45.07)	(39.89, 43.34, 45.50)
% of multiwavelength identifications	98.4%	98.1%	95.5%
% of z_{spec} (z_{adopted})[f]	67.2% (97.8%)	51.4% (93.4%)	47.5% (80.8%)
z_{adopted}	(0.000, 1.156, 5.776)	(0.000, 1.130, 5.365)	(0.000, 1.193, 7.203)
% of AGNs/galaxies/stars	70.5%/28.3%/1.2%	86.5%/11.0%/2.5%	90.6%/6.7%/2.7%
AGN/galaxy/star density (deg^{-2})[g]	13600/12100/250	12400/4200/100	5200/500/100

[a] For source properties, here we refer only to the main-catalog sources from Luo et al. (2017) and Xue et al. (2016).
[b] The E-CDF-S consists of four distinct, contiguous pointings that flank the CDF-S proper (see Fig. 1).
[c] P indicates the probability of a source not being real (i.e., due to background fluctuations).
[d] The three numbers in parentheses denote the minimum, median, and maximum values.
[e] This is the absorption-corrected rest-frame 0.5–7 keV luminosity.
[f] z_{adopted} denotes the adopted redshifts, with z_{spec} (spectroscopic redshifts) preferred over photometric redshifts.
[g] These are observed source densities calculated within the respective central $r \leq 3$ arcmin areas.

(All catalogs and relevant data products are publicly available!)

The 7 Ms CDF-S

(Xue, Luo, Brandt et al. 2011; Luo, Brandt, Xue et al. 2017)

- 102 observations over 16+ yrs
- Pencil-beam: ~484 arcmin^2
- Longest exposure (~81d)
- Most sensitive: 6.4E-18 cgs at SB; 1 photon/10 d
- 1055 X-ray sources
- Tremendous multi-wavelength investment

Spectroscopic data

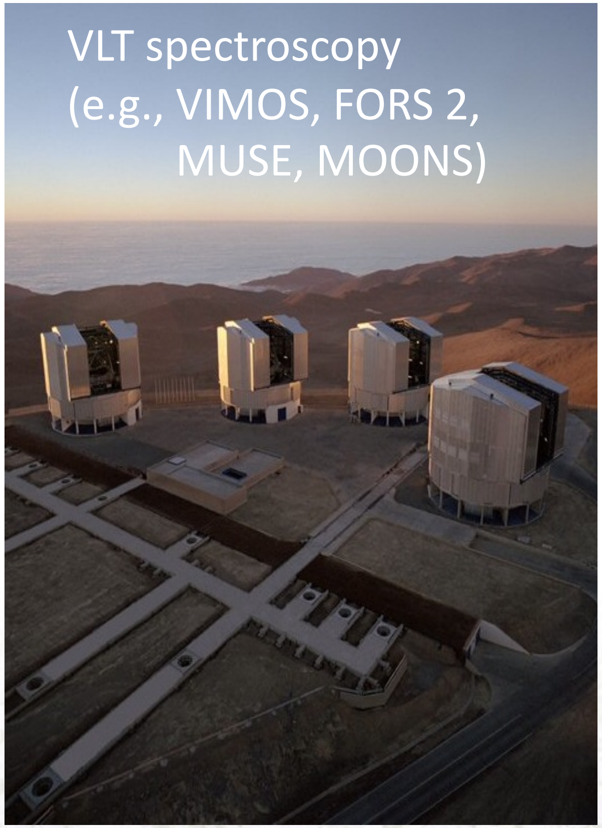

Enormous progress over the past 16 yr using multi-object spectrographs, but remains a persistent challenge and bottleneck (especially at faint fluxes).

Ultradeep multiwavelength coverage

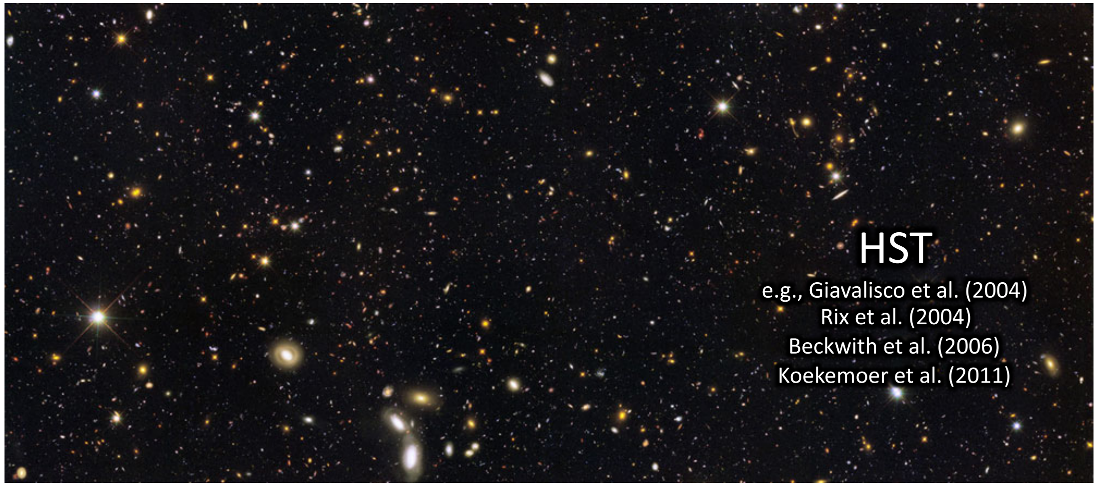

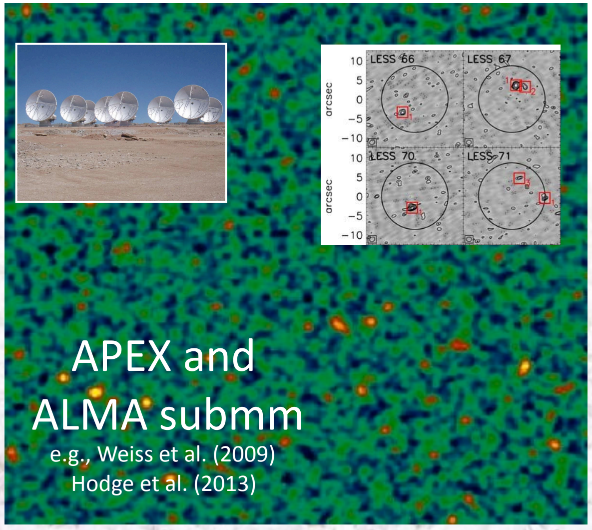

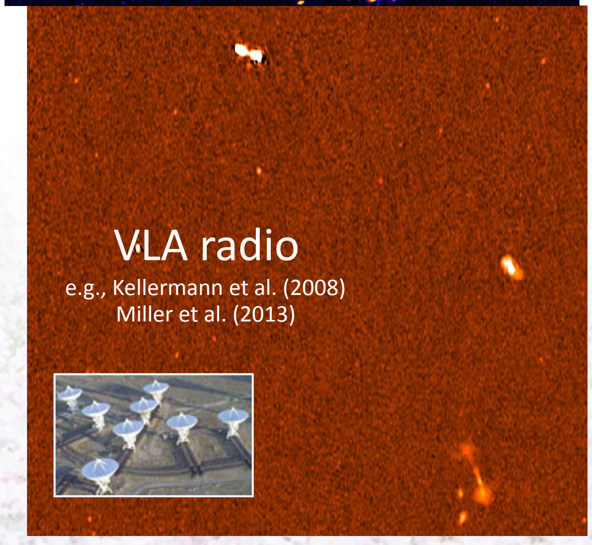

Critically important for source identification, source classification, host-galaxy measurements, etc.
Continues to improve rapidly, keeping the science exciting; e.g., MUSE, LMT, MOONS, JWST, LSST, ELTs.

Importance of multiwavelength data

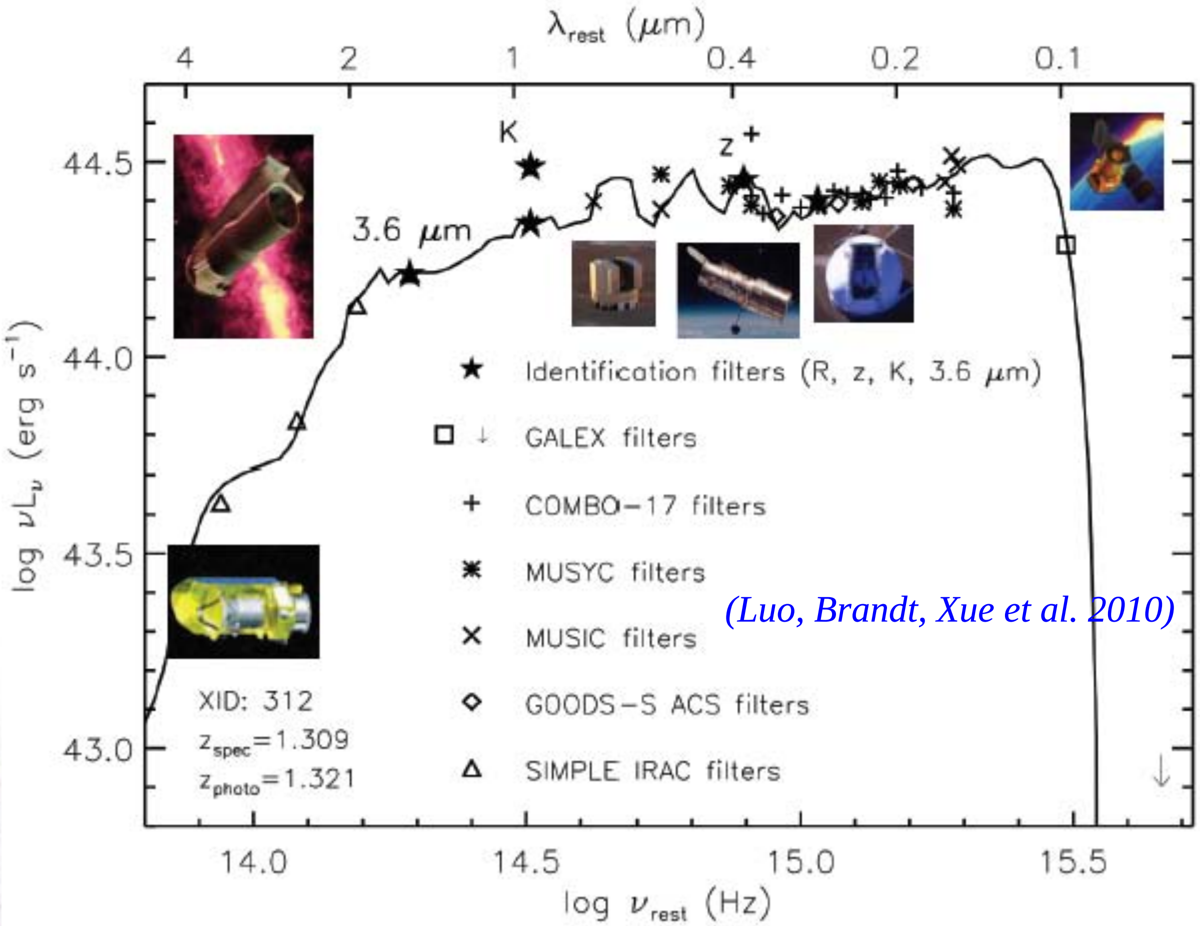

(Luo, Brandt, Xue et al. 2010)

- Source identification; spectroscopic and photometric redshifts
- Host-galaxy properties
- Large samples of non-active galaxies for comparison

中国科学技术大学
University of Science and Technology of China

CDF-N & H-HDF-N: photometric redshifts

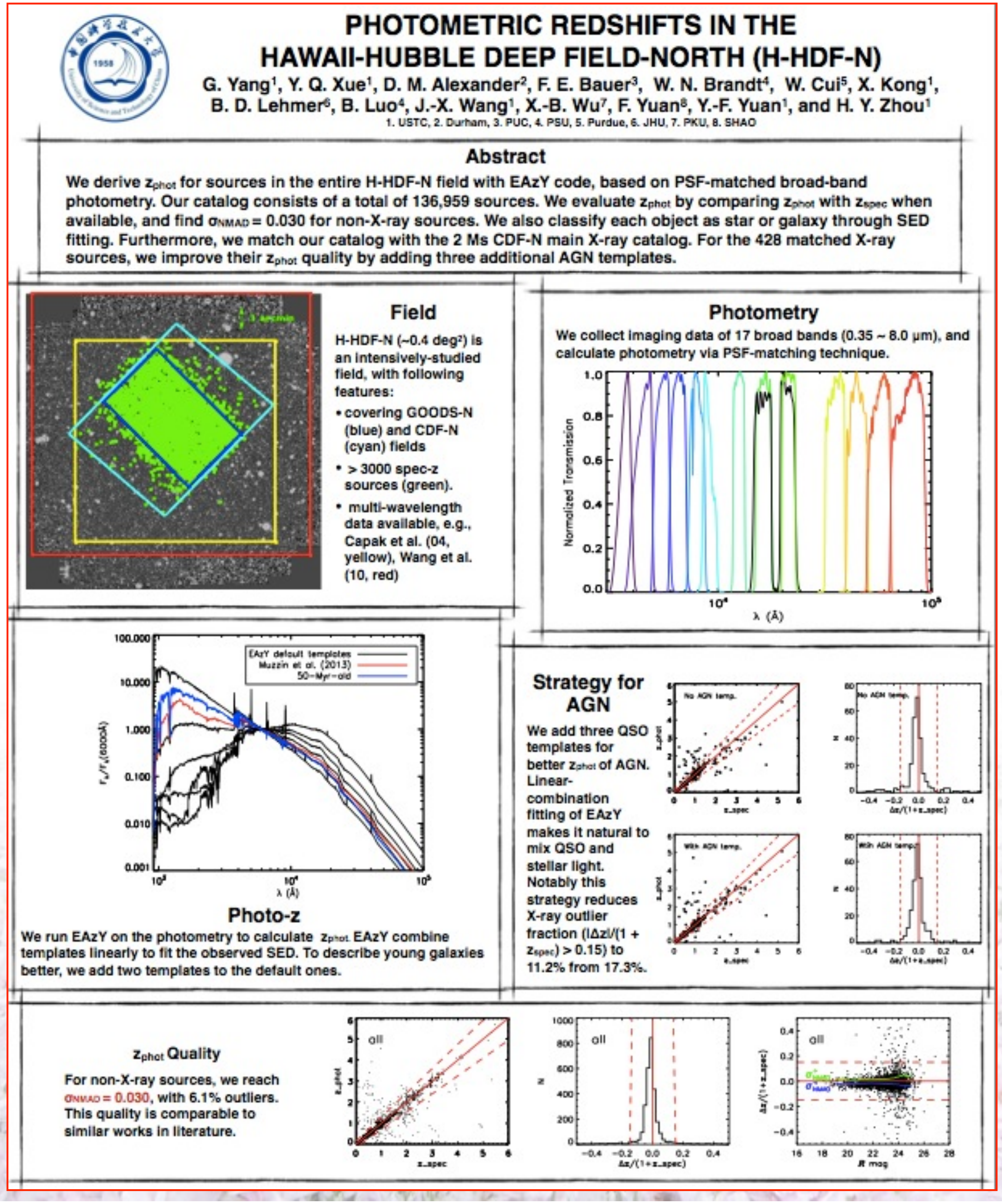

PHOTOMETRIC REDSHIFTS IN THE HAWAII-HUBBLE DEEP FIELD-NORTH (H-HDF-N)

G. Yang[1], Y. Q. Xue[1], D. M. Alexander[2], F. E. Bauer[3], W. N. Brandt[4], W. Cui[5], X. Kong[1], B. D. Lehmer[6], B. Luo[4], J.-X. Wang[1], X.-B. Wu[7], F. Yuan[8], Y.-F. Yuan[1], and H. Y. Zhou[1]

1. USTC, 2. Durham, 3. PUC, 4. PSU, 5. Purdue, 6. JHU, 7. PKU, 8. SHAO

Abstract

We derive z_{phot} for sources in the entire H-HDF-N field with EAzY code, based on PSF-matched broad-band photometry. Our catalog consists of a total of 136,959 sources. We evaluate z_{phot} by comparing z_{phot} with z_{spec} when available, and find σ_{NMAD} = 0.030 for non-X-ray sources. We also classify each object as star or galaxy through SED fitting. Furthermore, we match our catalog with the 2 Ms CDF-N main X-ray catalog. For the 428 matched X-ray sources, we improve their z_{phot} quality by adding three additional AGN templates.

Field

H-HDF-N (~0.4 deg²) is an intensively-studied field, with following features:

- covering GOODS-N (blue) and CDF-N (cyan) fields
- > 3000 spec-z sources (green).
- multi-wavelength data available, e.g., Capak et al. (04, yellow), Wang et al. (10, red)

Photometry

We collect imaging data of 17 broad bands (0.35 ~ 8.0 μm), and calculate photometry via PSF-matching technique.

Photo-z

We run EAzY on the photometry to calculate z_{phot}. EAzY combine templates linearly to fit the observed SED. To describe young galaxies better, we add two templates to the default ones.

Strategy for AGN

We add three QSO templates for better z_{phot} of AGN. Linear-combination fitting of EAzY makes it natural to mix QSO and stellar light. Notably this strategy reduces X-ray outlier fraction ($|\Delta z|/(1 + z_{spec}) > 0.15$) to 11.2% from 17.3%.

z_{phot} Quality

For non-X-ray sources, we reach σ_{NMAD} = 0.030, with 6.1% outliers. This quality is comparable to similar works in literature.

(Yang, Xue et al. 2014)

University of Science and Technology of China

中国科学技术大学


Chandra Deep Field South
Optical

4 Ms CDF-S: record AGN number counts

AGN: 14900/deg^2

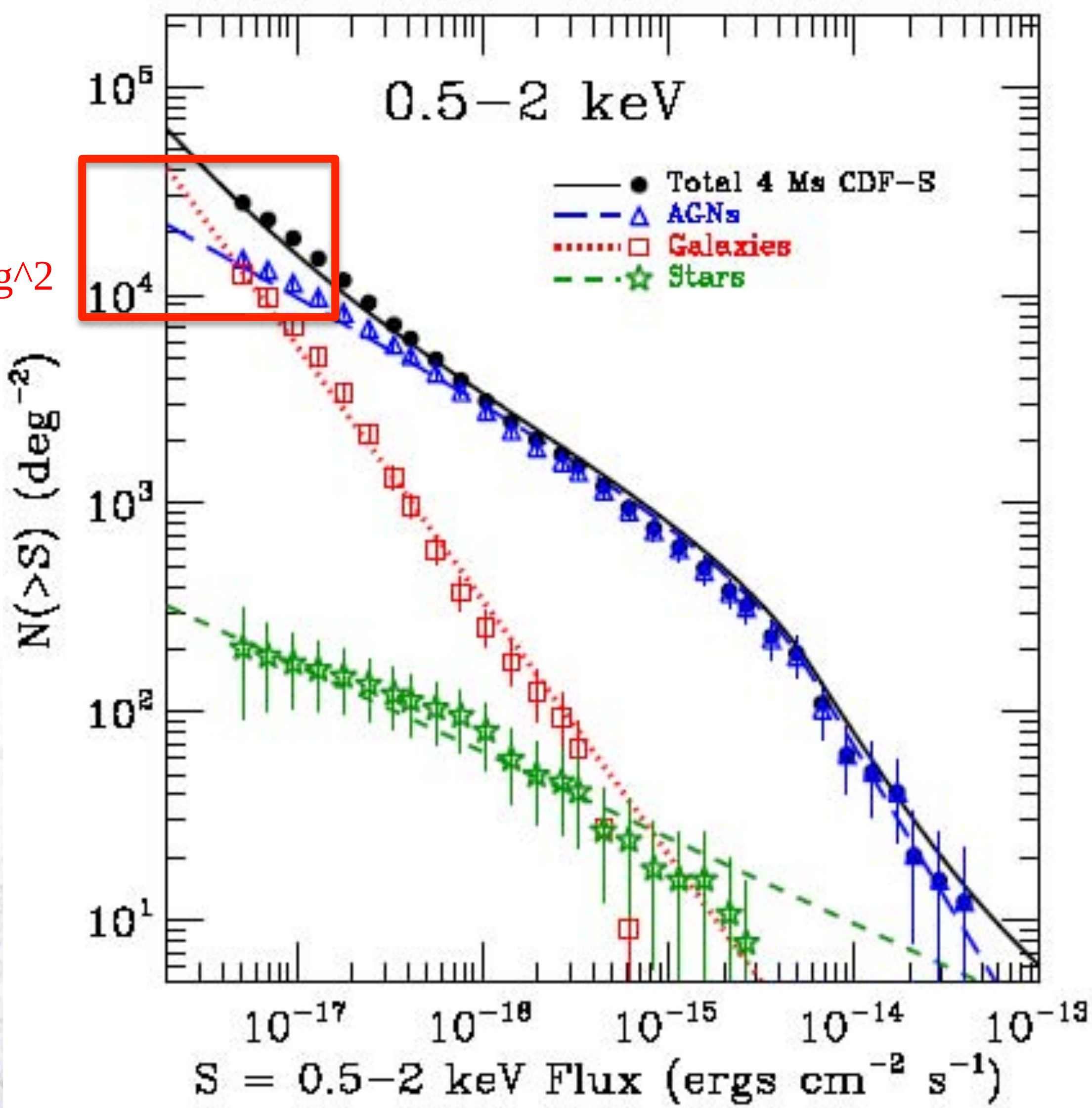

(Lehmer, Xue, Brandt, et al. 2012)

4 Ms CDF-S: AGN number counts

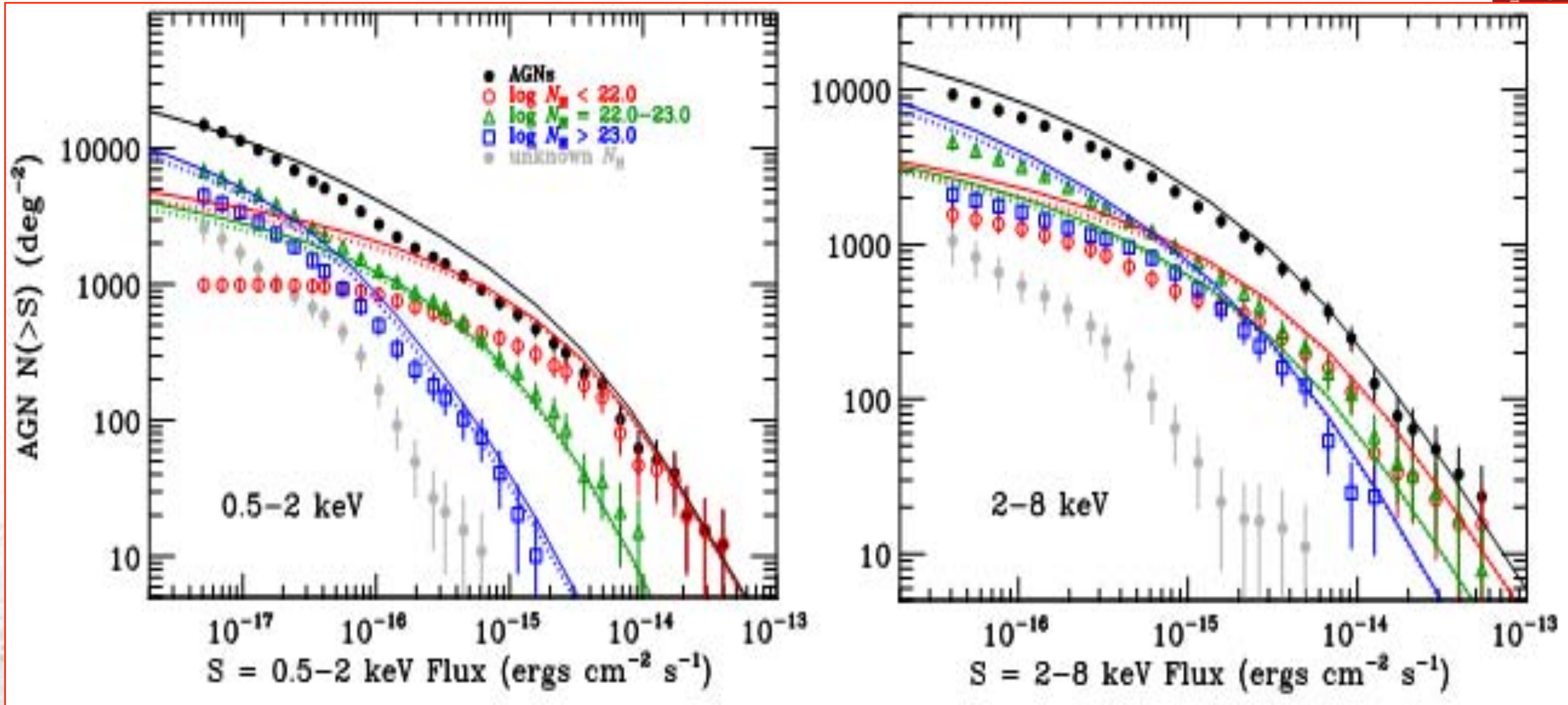

(Lehmer, Xue, Brandt, et al. 2012)

7 Ms CDF-S: record AGN number counts

AGN: 23900/deg^2

→1 billion AGNs in the entire sky

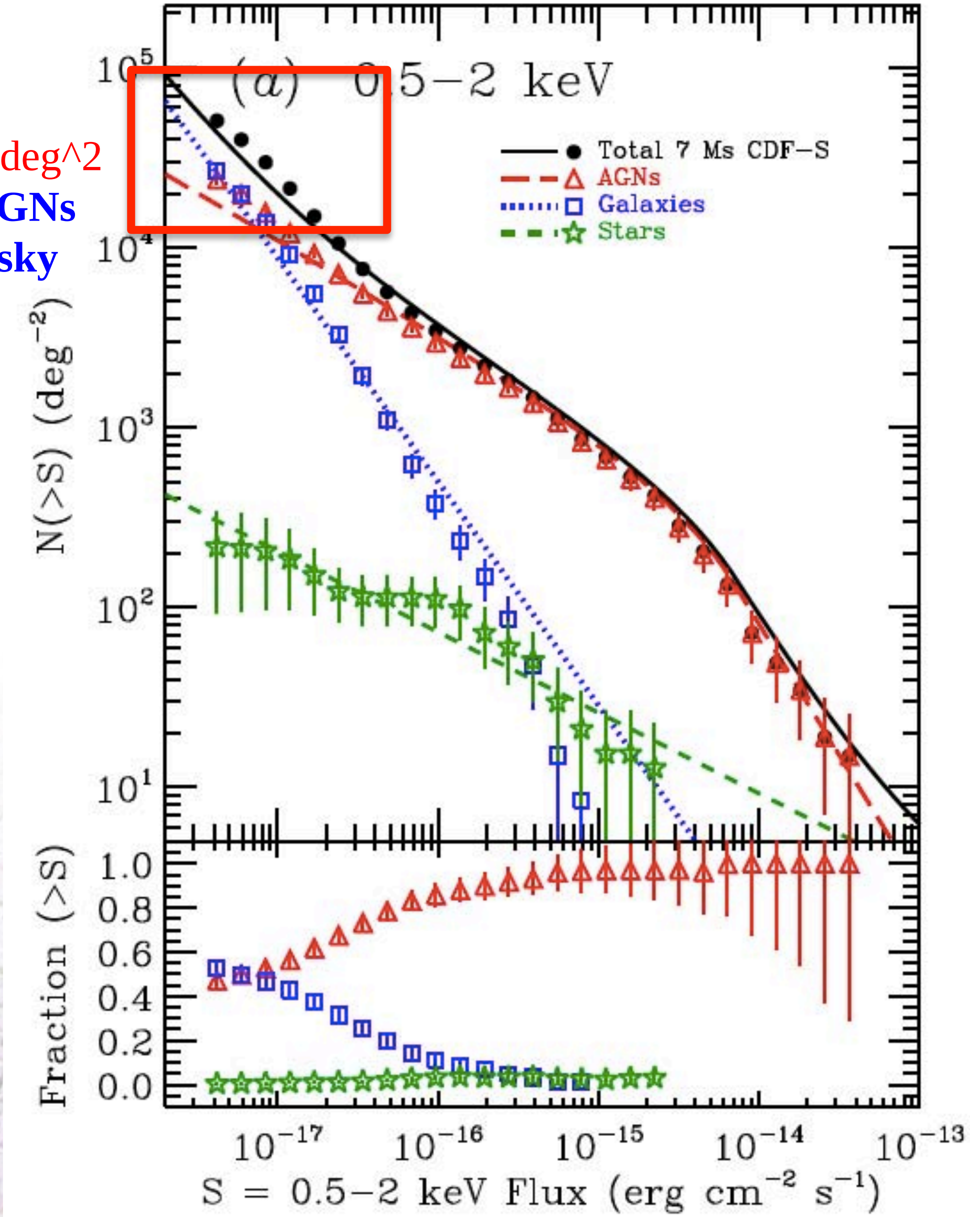

(Luo, Brandt, Xue et al. 2017)

University of Science and Technology of China

中国科学技术大学

4 Ms CDF-S: z=4.76 CT-AGN

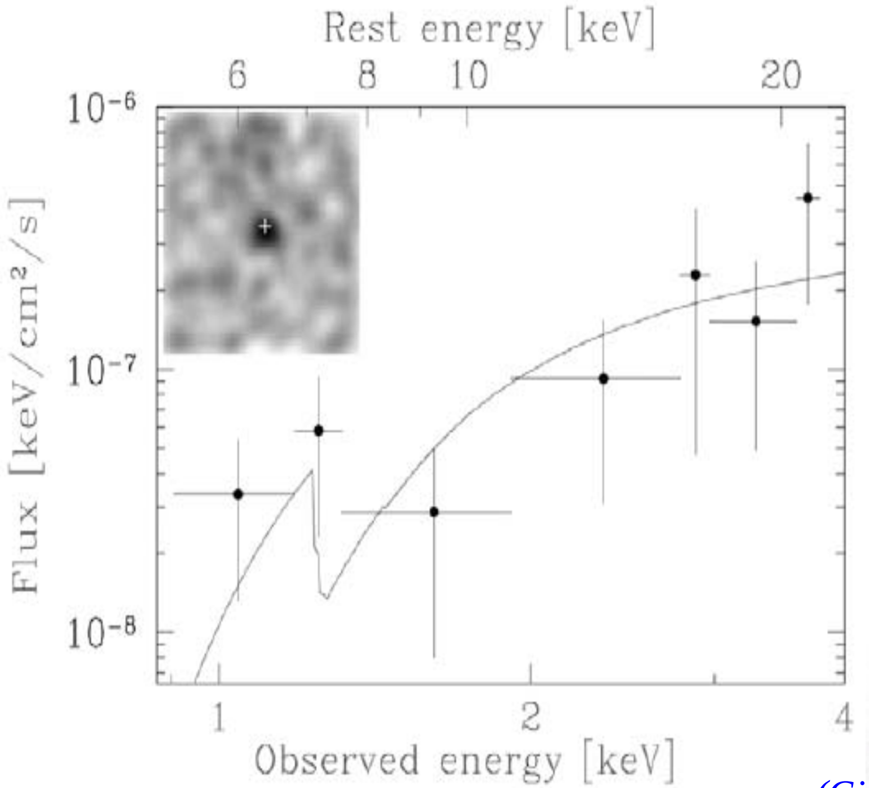

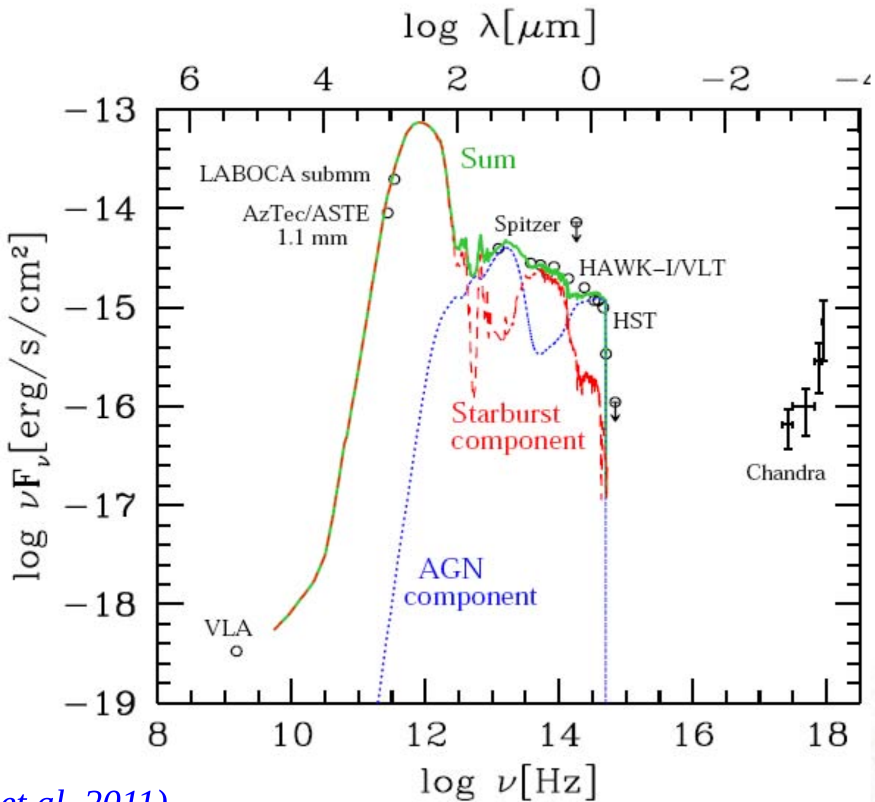

(Gilli et al. 2011)

- Compton-thick AGN plus strongly star-forming host
- Key phase in SMBH/galaxy co-evolution where obscured SMBH rapidly growing in forming bulge
- Measuring number density of such AGNs crucial to reconstruct early co-evolution history

4 Ms CDF-S: z~2 highly obscured AGNs

222 K<22, z~2 *BzK*-selected galaxies in central CDF-S

47 (~21%) X-ray detected

11 highly obscured

36 unobscured/starbursts

7 IR-excess galaxies

prefer pure reflection model

reflection-dominated composite spectrum

(Alexander et al. 2011)

4 Ms CDF-S: *z*~2 highly obscured AGNs

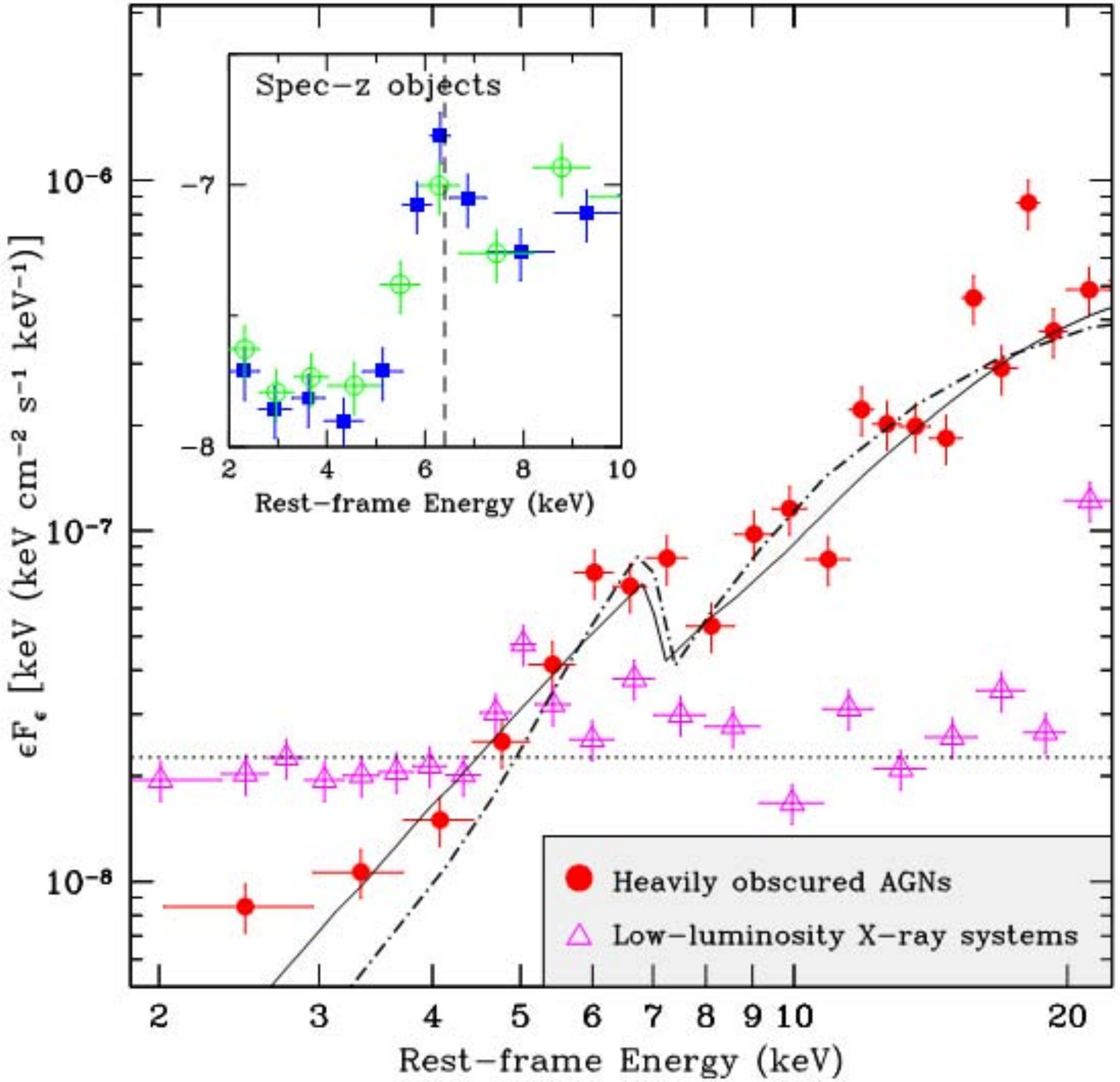

(Alexander et al. 2011)

4 Ms CDF-S: *z*~2 highly obscured AGNs

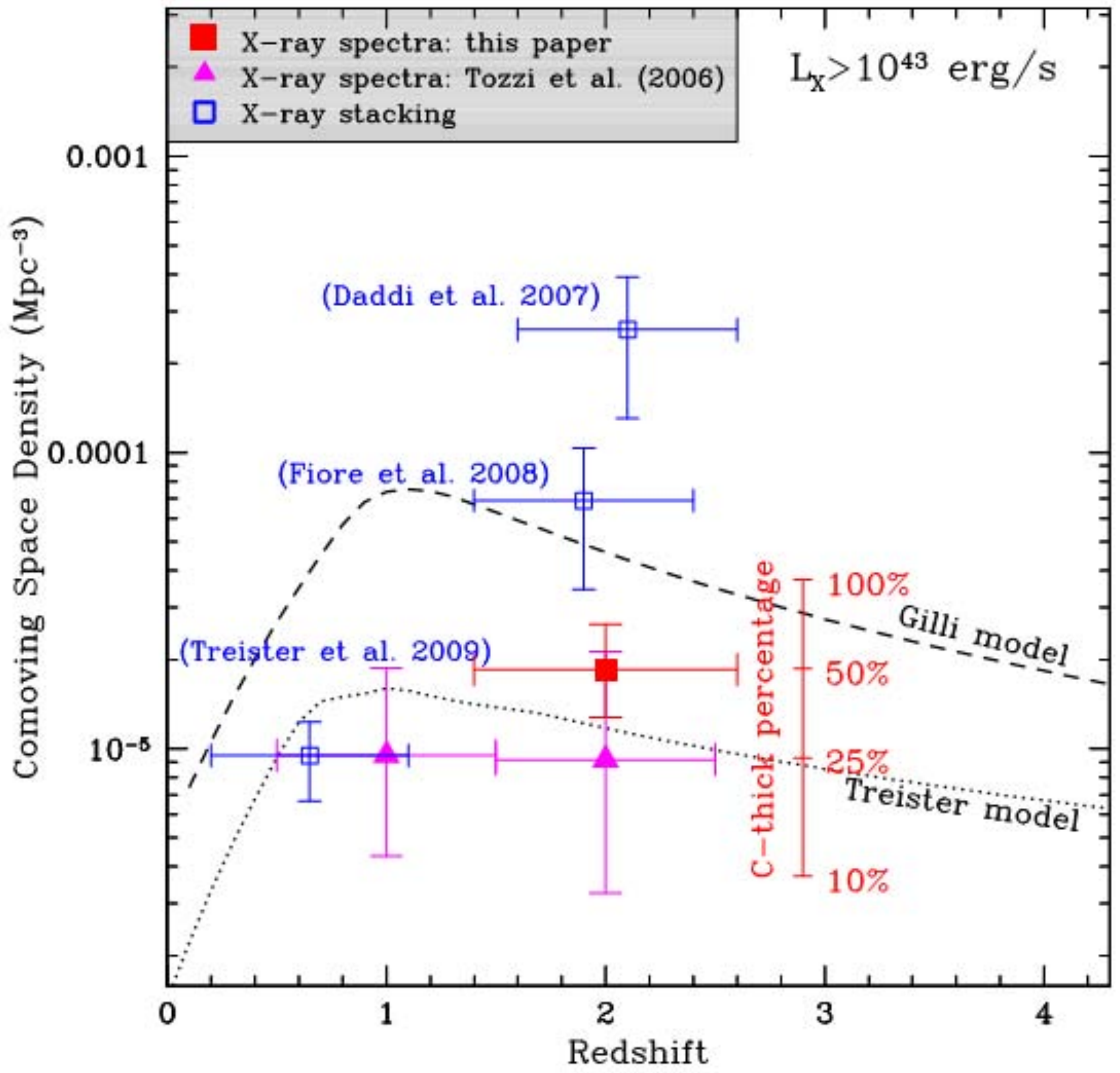

(Alexander et al. 2011)

4 Ms CDF-S: *z*~0.5-1 highly-obs. AGNs

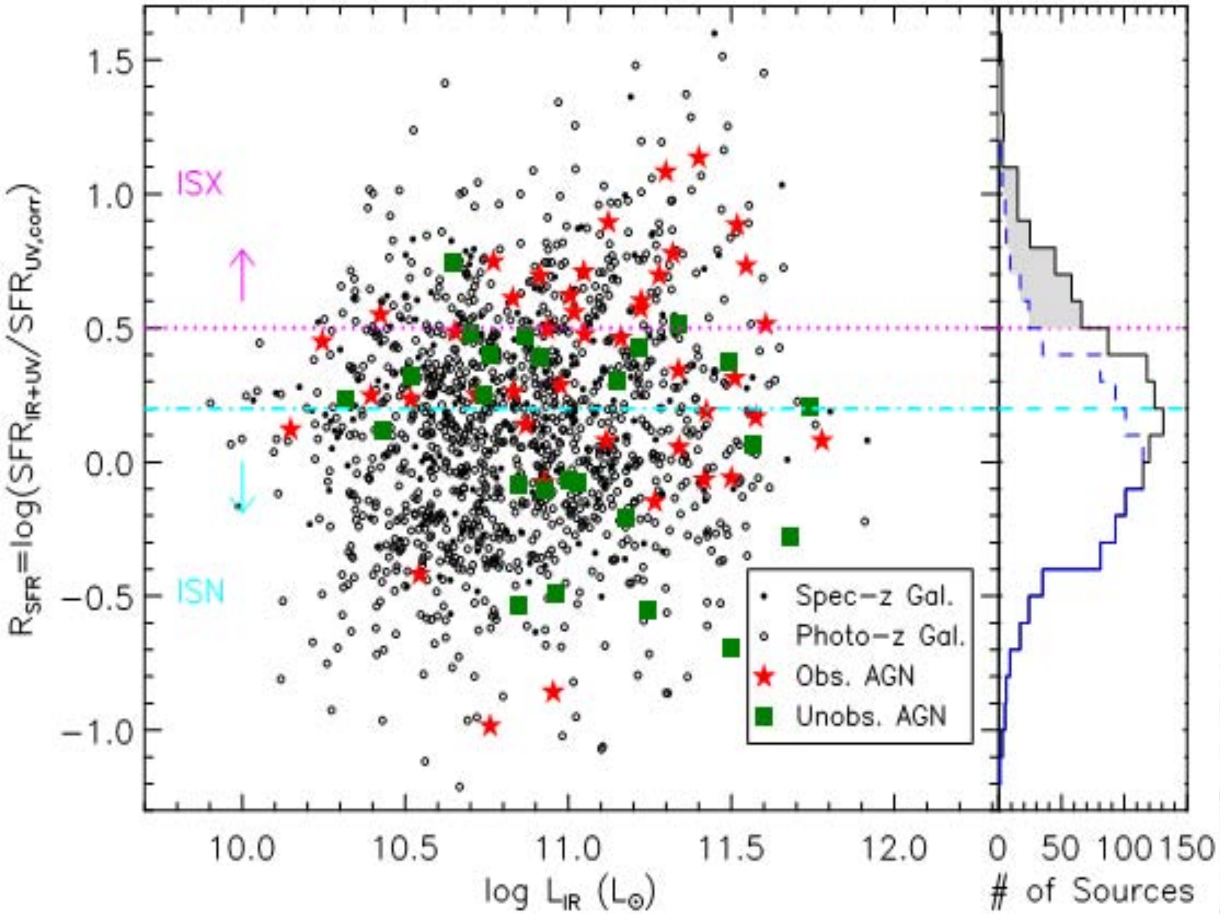

23 ISX sources:

- z=0.5-1
- MIPS detected
- >10 opt. filters
- >5E9 Msun
- X-ray not detected
- no X-ray src nearby
- IR-excess
- theta<6 arcmin

(Luo, Brandt, Xue et al. 2011)

4 Ms CDF-S: *z*~0.5-1 highly-obs. AGNs

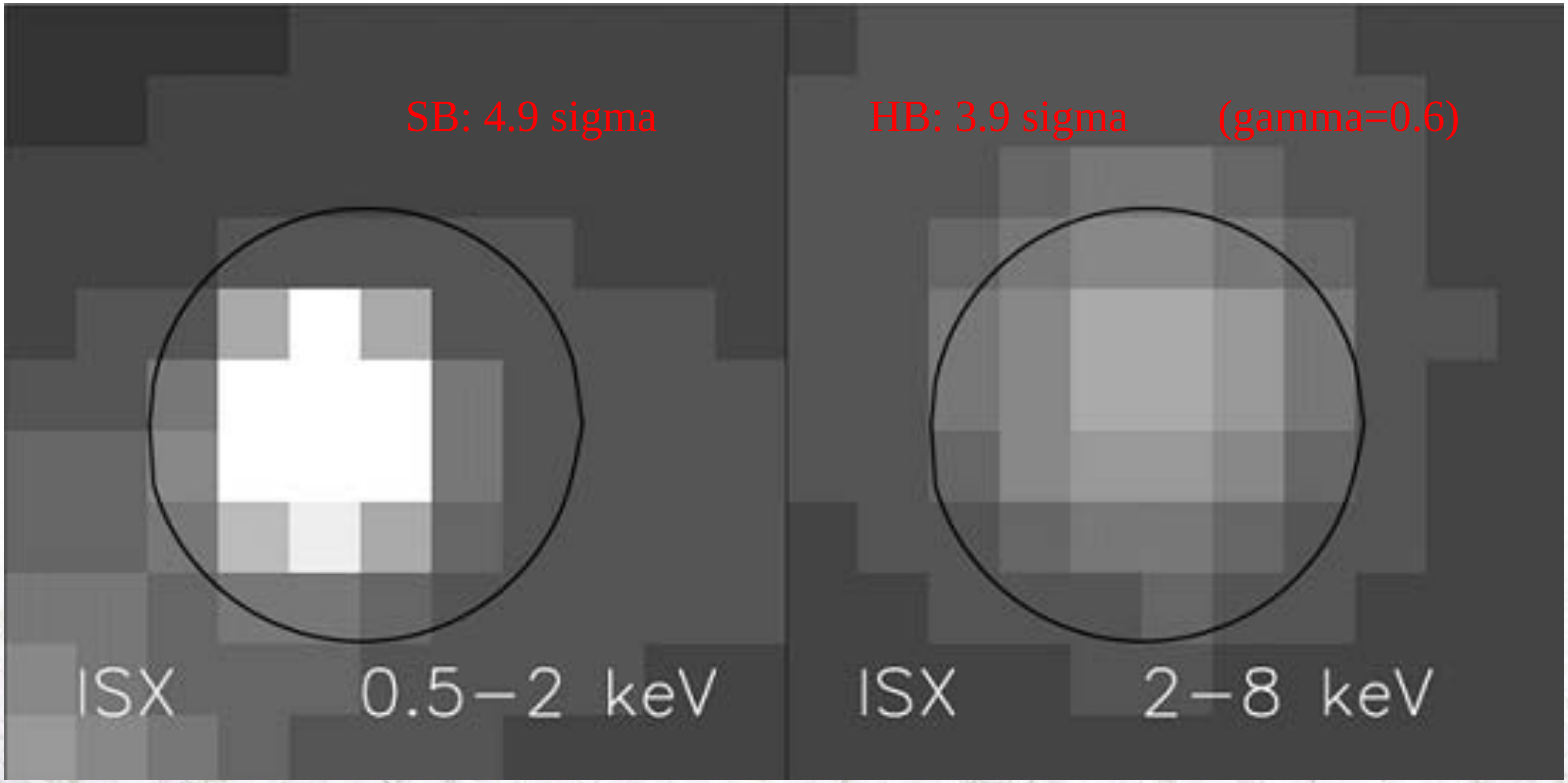

(Luo, Brandt, Xue et al. 2011)

4 Ms CDF-S: z~0.5-1 highly-obs. AGNs

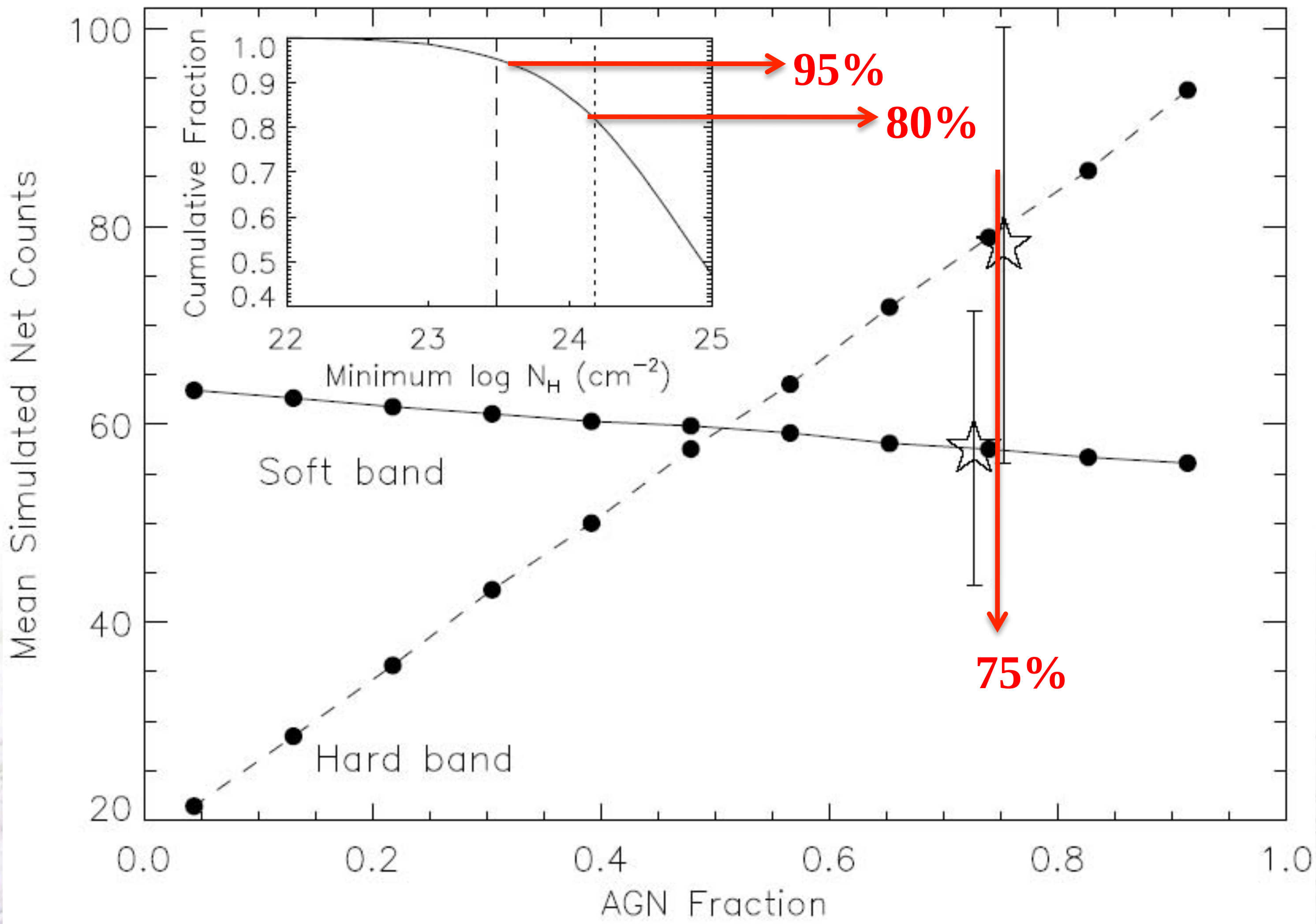

(Luo, Brandt, Xue et al. 2011)

4 Ms CDF-S: z~0.5-1 highly-obs. AGNs

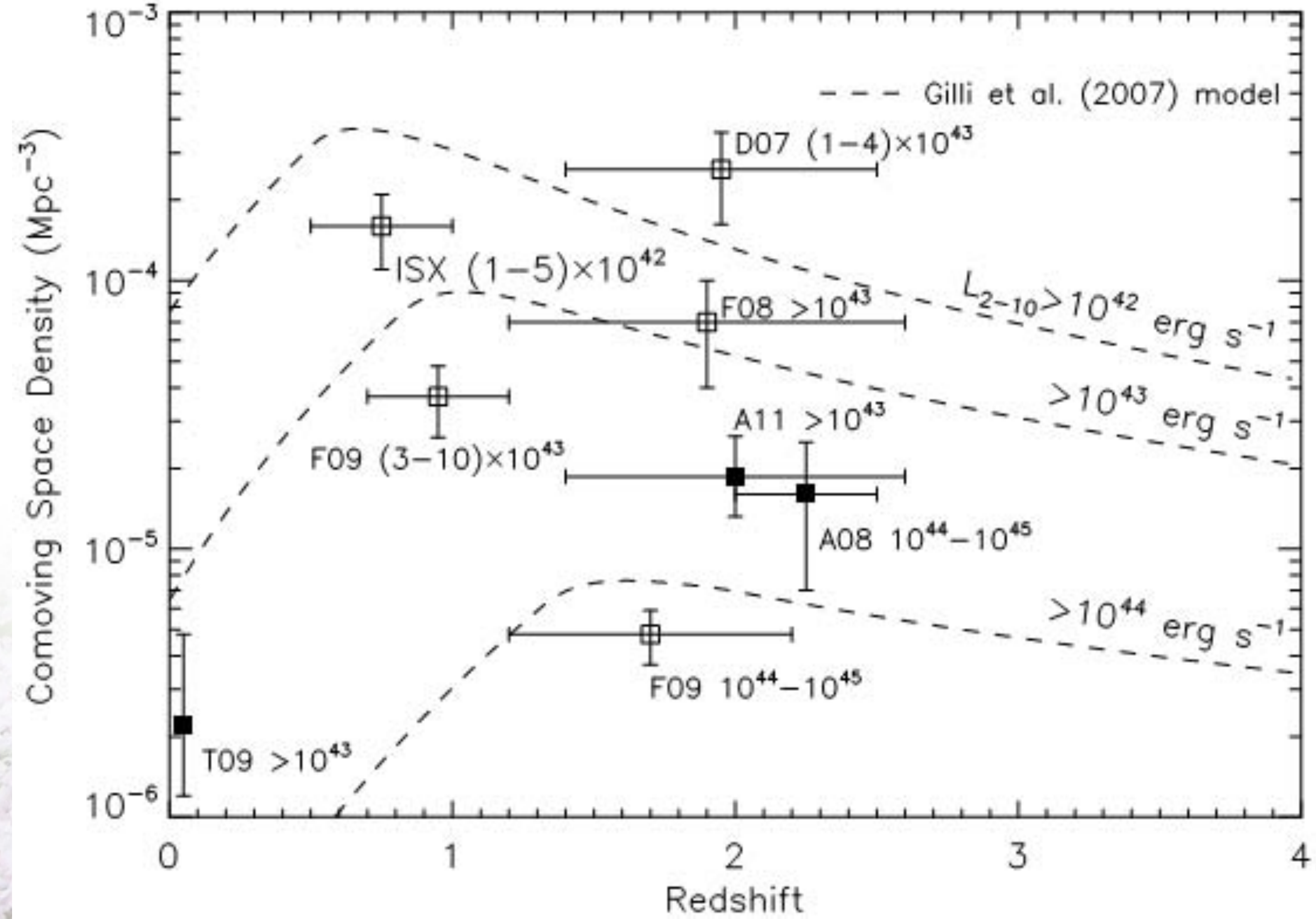

(Luo, Brandt, Xue et al. 2011)

4 Ms CDF-S: *z*~0.5-1 highly-obs. AGNs

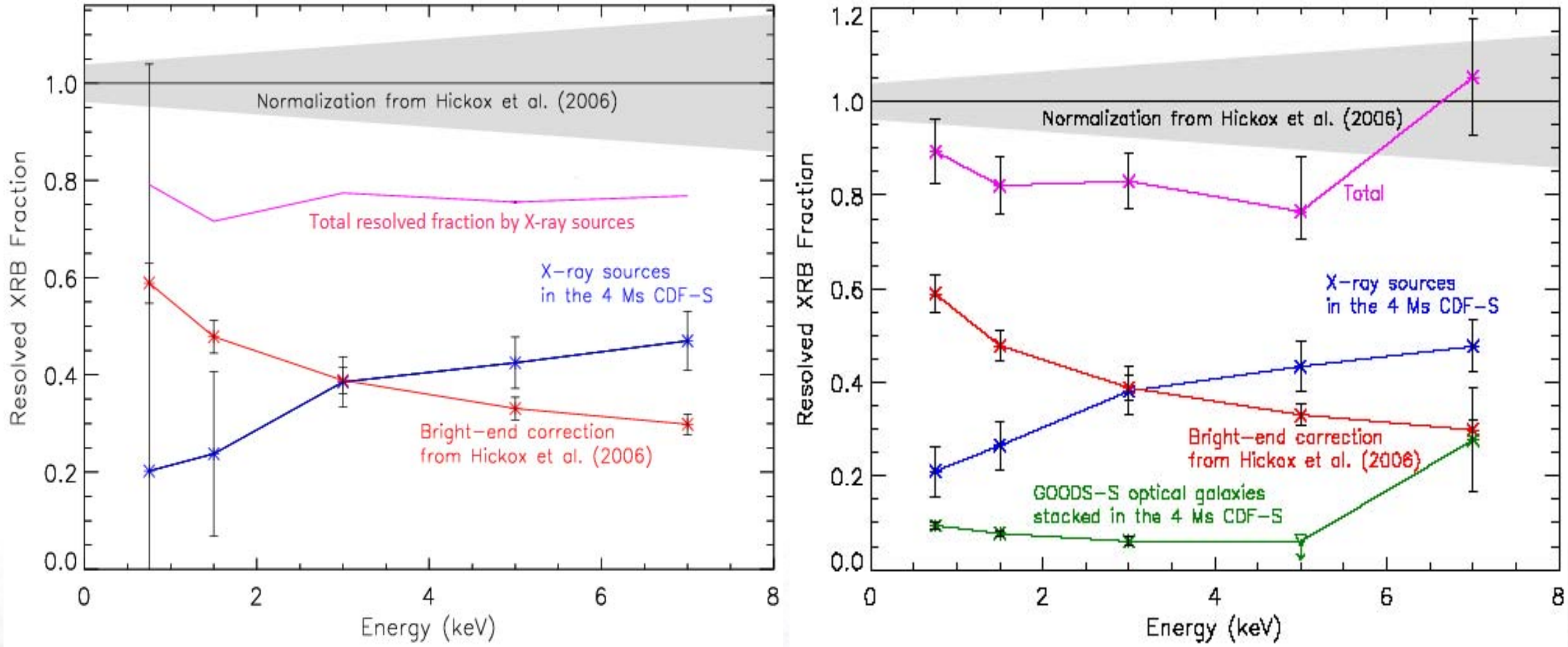

(Luo, Brandt, Xue et al. 2011)

- CXRB resolved fraction roughly constant (~80%)
- Minor contribution from ISX sources (<5% of unresolved 6-8 keV emission)
- Unresolved 0.5-6 keV fraction: cosmic variance? extended X-ray emission?
- Unresolved 6-8 keV fraction: missing Compton-thick population?

University of Science and Technology of China 中国科学技术大学

4 Ms CDF-S: src for rest 6-8 keV emission?

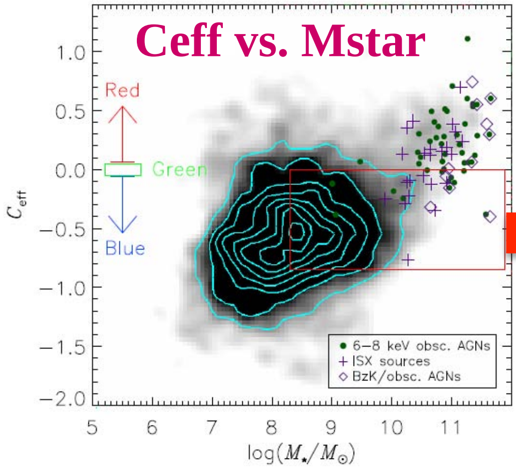

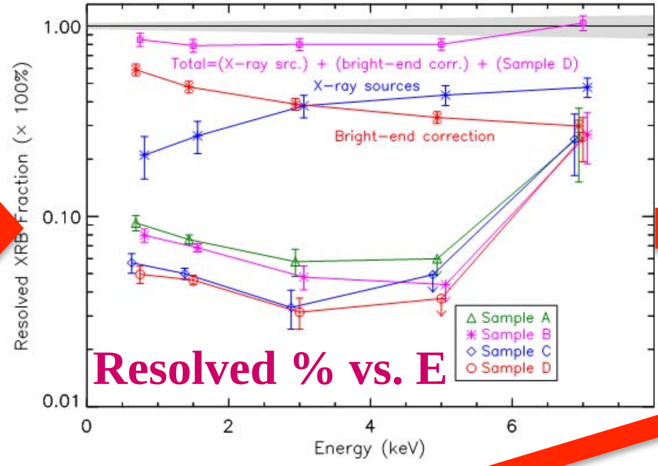

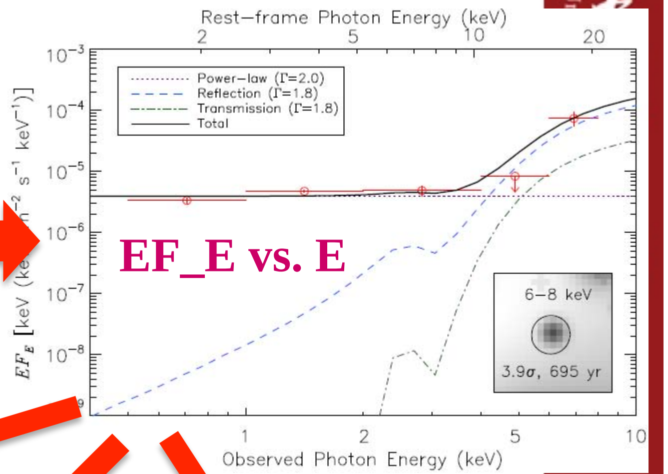

Resl. 6-8keV % vs. z

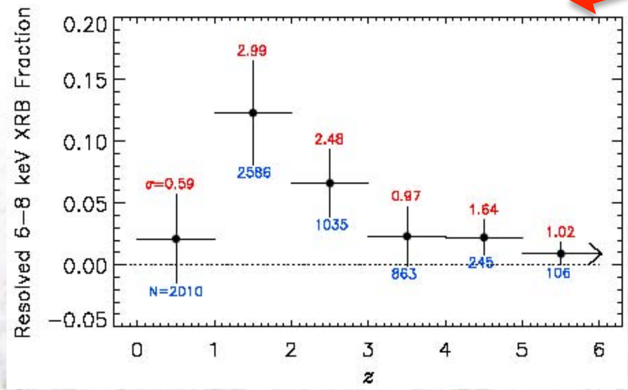

vs. mag

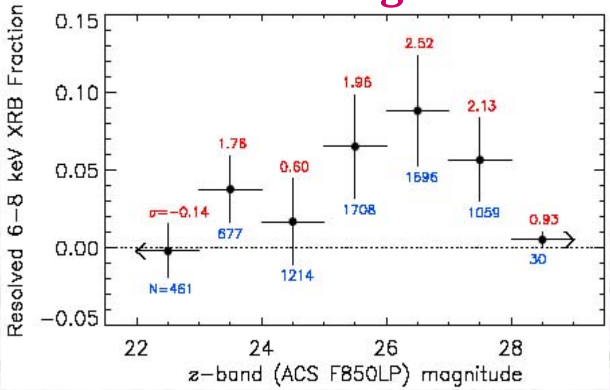

vs. Mstar

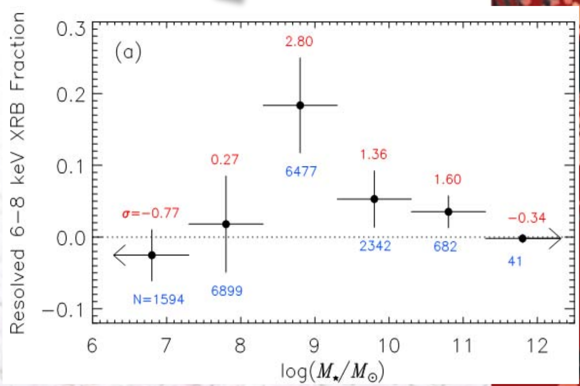

(Xue, Wang, Brandt et al. 2012)

- Source population responsible for the unresolved 6-8 keV CXRB: top of blue cloud, 1<z<3, 25<z_850<28, 2e8<M_stellar/M_sun<2e9!

GOODS-Herschel: a large pop. of MIR luminous, heavily-obscured, CT quasars at z~1-3

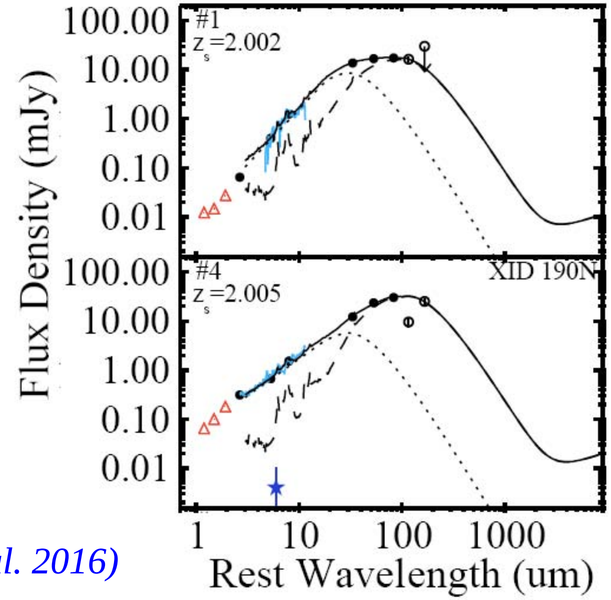

(Del Moro et al. 2016)

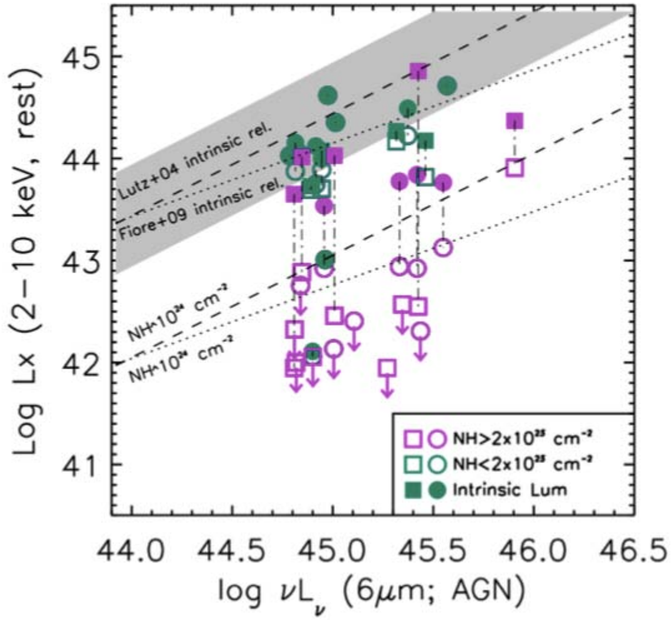

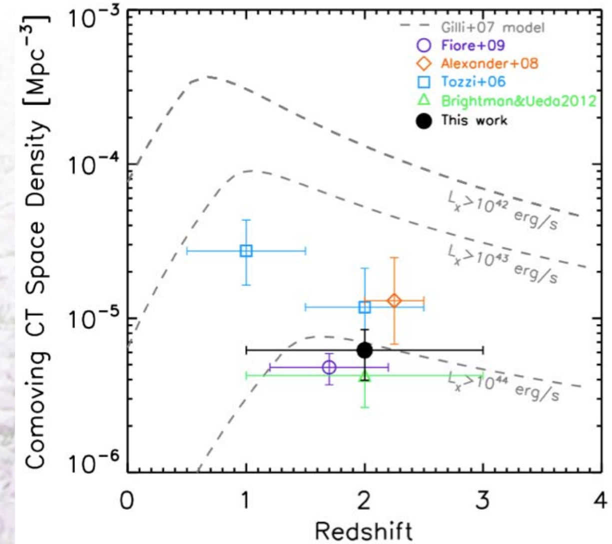

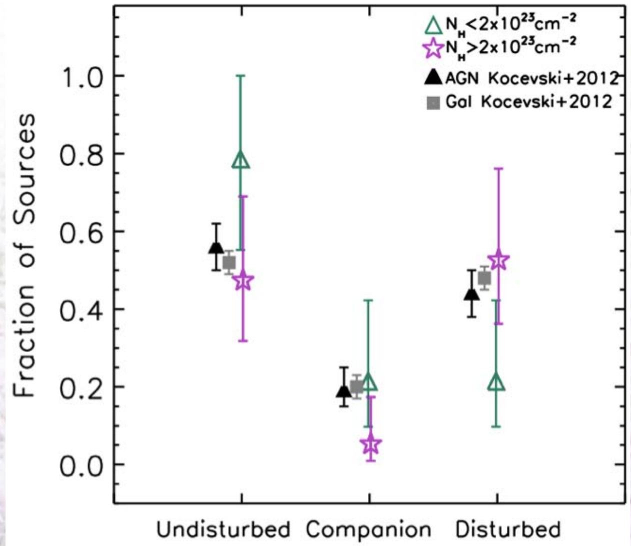

Outline

- Highly-obscured/Compton-thick AGNs
- Recent efforts in searching for these AGNs in the CDF-S
- Summary
- Prospects

中国科学技术大学
University of Science and Technology of China

- Highly-obscured/CT AGNs: required by AGN synthesis model for XRB; predicted to be numerous and ubiquitous
- Only a small fraction detected/identified on cosmological distances
  - --- (1) record AGN number counts
  - --- (2) a z=4.76 CT-AGN
  - --- (3) z~2 highly-obscured AGNs
  - --- (4) z~0.5-1 highly-obscured AGNs
  - --- (5) source population responsible for unresolved 6-8 keV XRB
  - --- (6) $1<z<3$ MIR luminous, highly-obscured, CT quasars
- Missed highly obscured AGNs and their contribution to SMBH growth
- At high z, even a small number of such objects can provide critical leverage in modeling early SMBH growth

Outline

- Highly-obscured/Compton-thick AGNs
- Recent efforts in searching for these AGNs in the CDF-S
- Summary
- Prospects

  - extensive and effective exploitation of CDF-S data

  - great future field: Wide CDF-S area (W-CDF-S)

中国科学技术大学

University of Science and Technology of China

THE EVOLUTION OF NORMAL GALAXY X-RAY EMISSION THROUGH COSMIC HISTORY: CONSTRAINTS FROM THE 6 MS *CHANDRA* DEEP FIELD-SOUTH

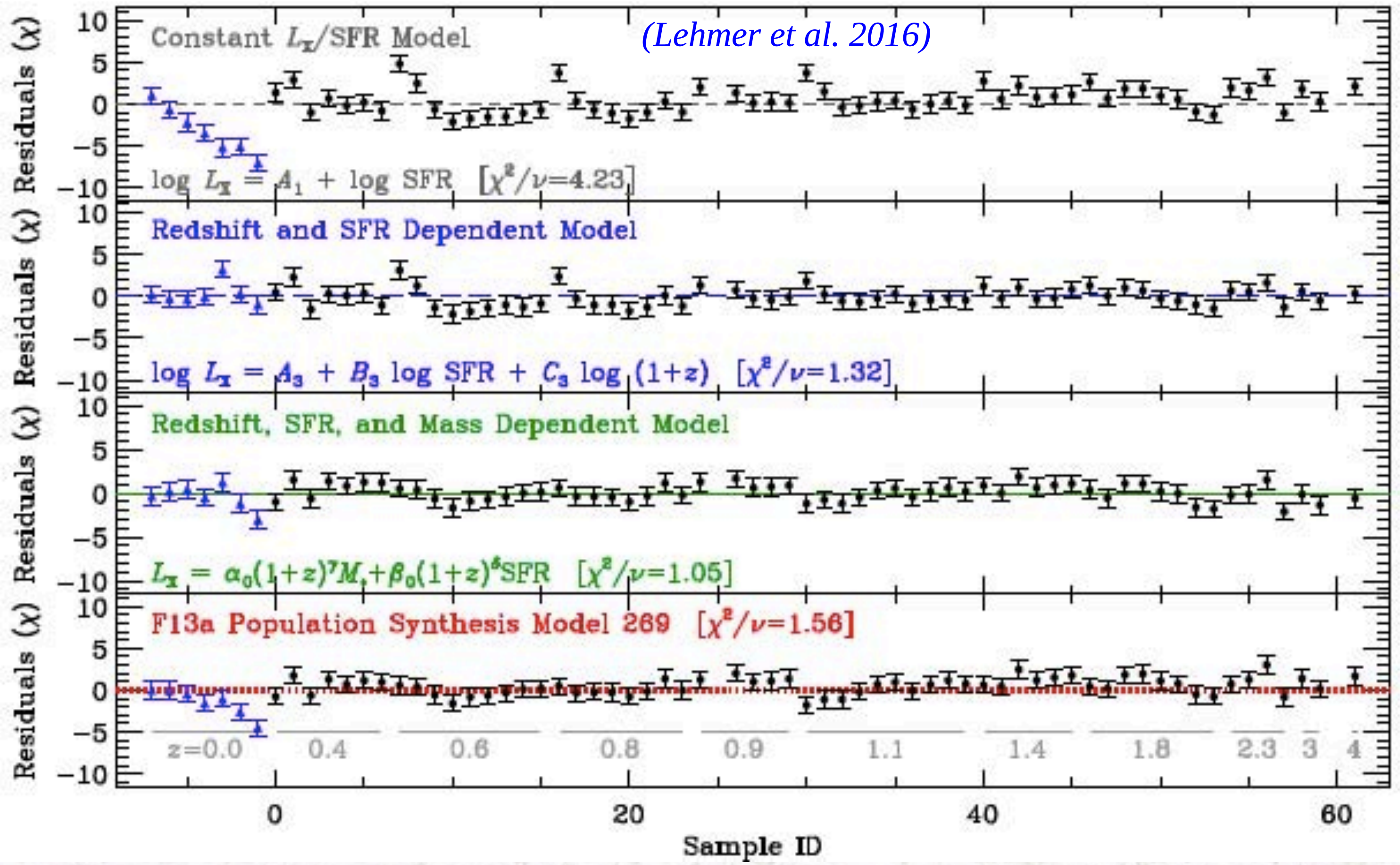

- Scaling relations involving SFR, M*, and z (vs. SFR only): better characterize average X-ray emission of normal galaxy populations at z~0-7
- First empirical constraints on z evolution of LMXB and HMXB X-ray emission:

$$L_{2-10\,\mathrm{keV}}(\mathrm{LMXB})/M_\star \propto (1+z)^{2-3} \text{ and } L_{2-10\,\mathrm{keV}}(\mathrm{HMXB})/\mathrm{SFR} \propto (1+z)$$

- Emission from XRBs could provide an important source of heating to IGM in early universe, exceeding that of AGNs

The deepest X-ray view of high-redshift galaxies: constraints on low-rate black hole accretion

(Vito et al. 2016)

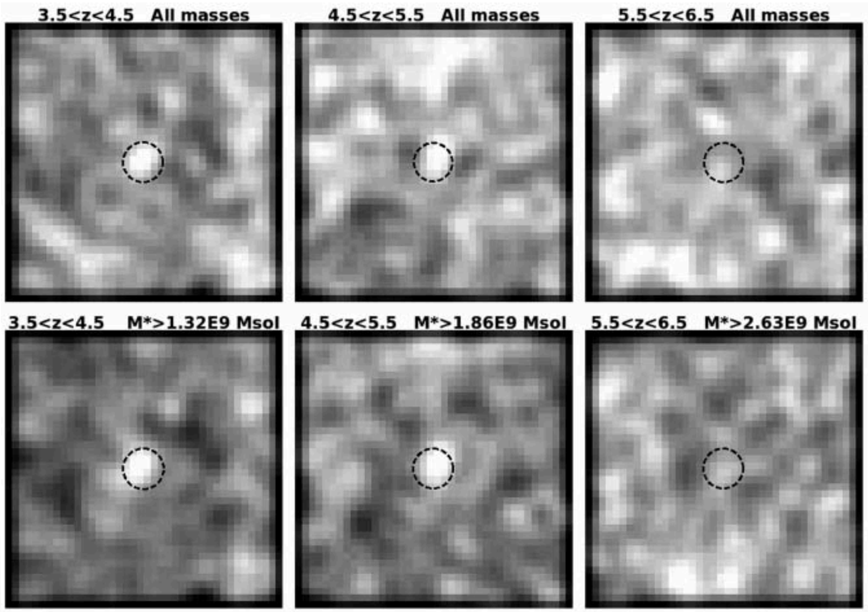

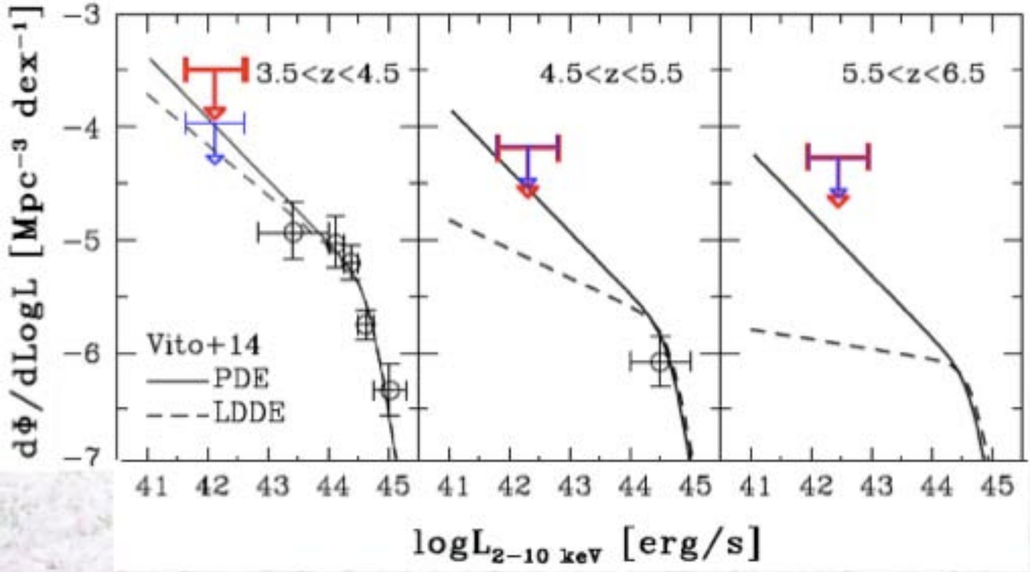

- Most sensitive stacking of X-ray emission from high-z (3.5<z<6.5) massive galaxies:
  - >3.7 sigma at z~4; 2.7 sigma at z~5 (highest sig. in such z); no sig. at even higher z
- These high-z X-ray signals mostly due to SF; negligible low-rate BH accretion compared to X-ray detected AGNs at high z
- First constraints on faint-end (Lx~1e42) of AGN XLF at z>4 (fairly flat slopes)

LONG-TERM X-RAY VARIABILITY OF TYPICAL ACTIVE GALACTIC NUCLEI IN THE DISTANT UNIVERSE

(Yang et al. 2016)

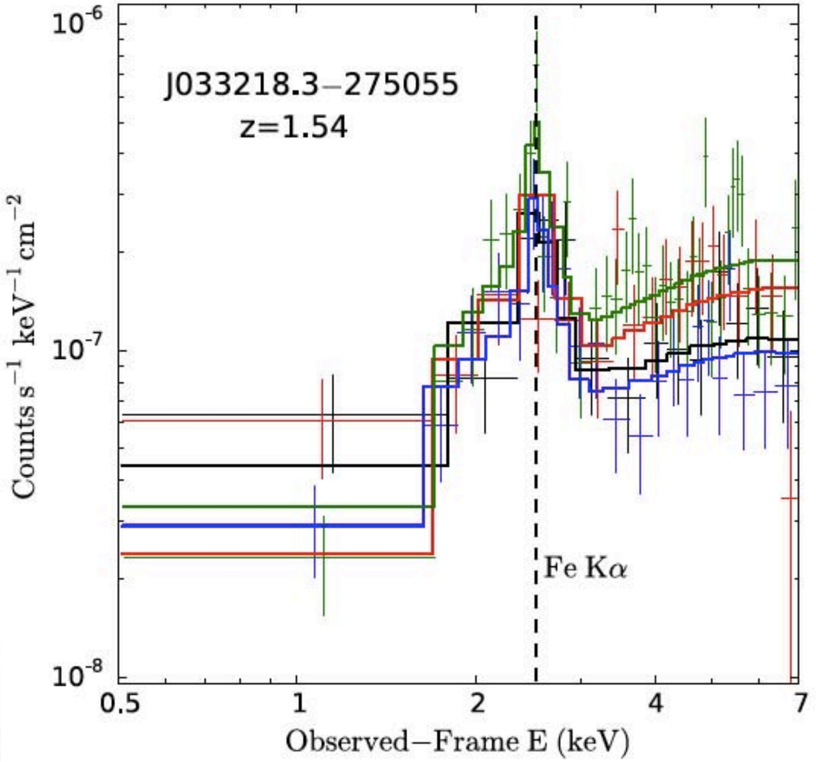

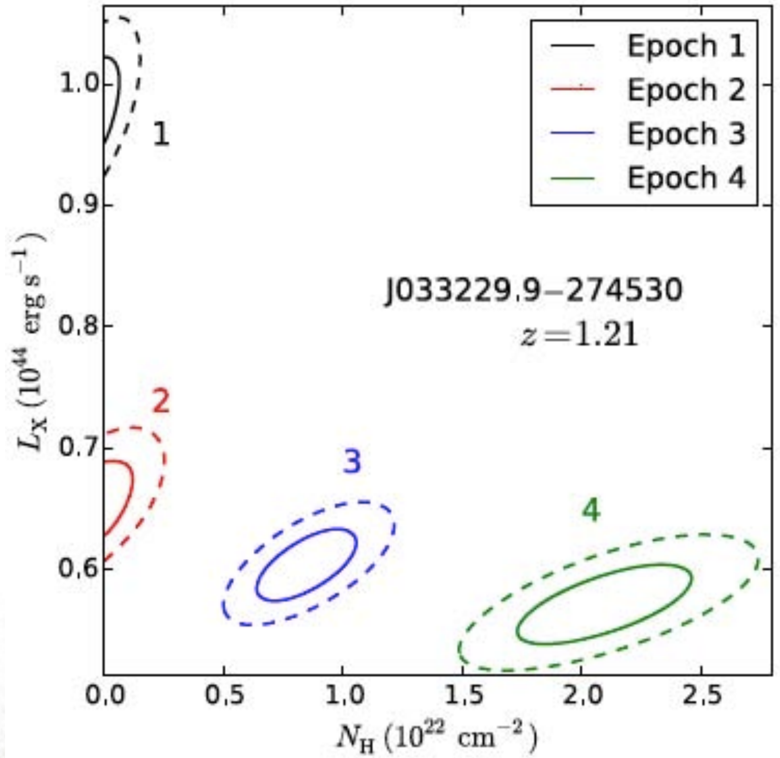

- Longest timescales probed for X-ray variabilities of distant AGNs
  - photometric analyses: widespread (90%) photon flux variability
  - spectral fitting: 74% show Lx variability, 16% show nH variability
- A CTAGN: high-E X-ray flux variation → size of reflecting material <~0.3 pc
- An AGN: X-ray unobscured → obscured while always being optical type I

PRELIMINARY RESULTS OF X-RAY VARIABILITY IN THE CHANDRA DEEP FIELD-SOUTH

X. C. Zheng, Y. Q. Xue, W. N. Brandt, G. Yang, S. F. Zhu, B. Luo, M. Y. Sun, F. Vito and friends.

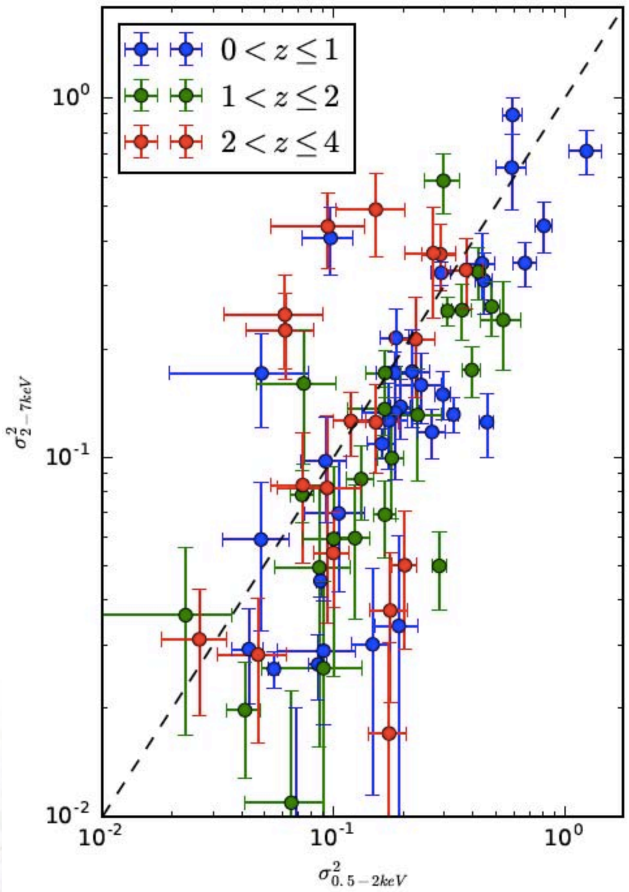

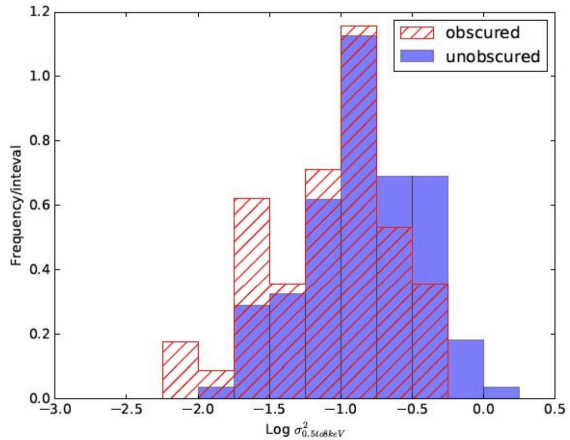

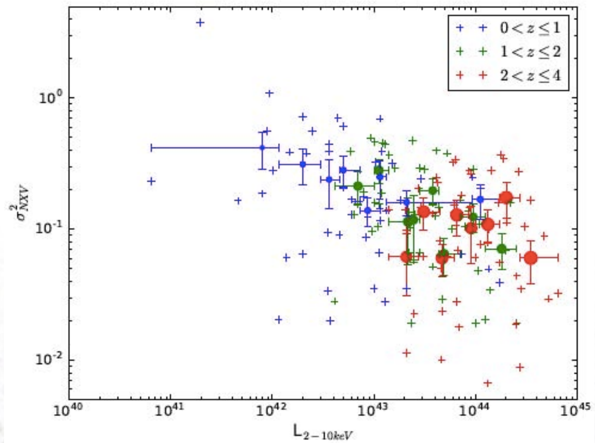

- Analyze X-ray variability of AGNs in the 7Ms CDF-S: *(Zheng, Xue, et al., in prep.)*
  - X-ray variable amplitude seems to be stronger in the softer band
  - no difference of variability is detected between obscured and unobscured samples
  - negative correlation between normalized excess variance and X-ray luminosity, which can be explained by a broken power-law PSD model with beta~1.2 below f_br

中国科学技术大学
University of Science and Technology of China

Census of highly-obscured AGNs in CDFs

(Li, Xue, et al., in prep.)

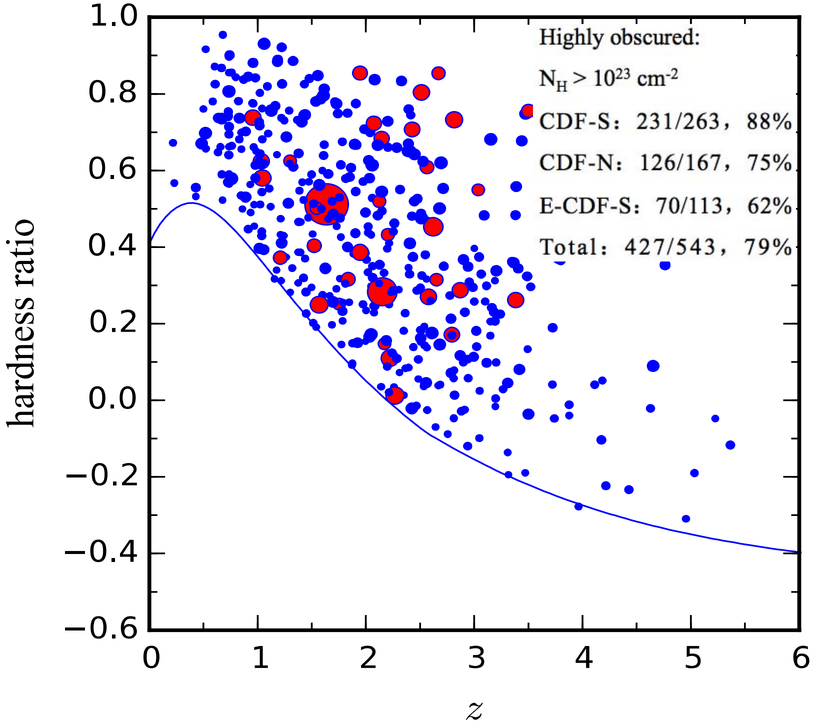

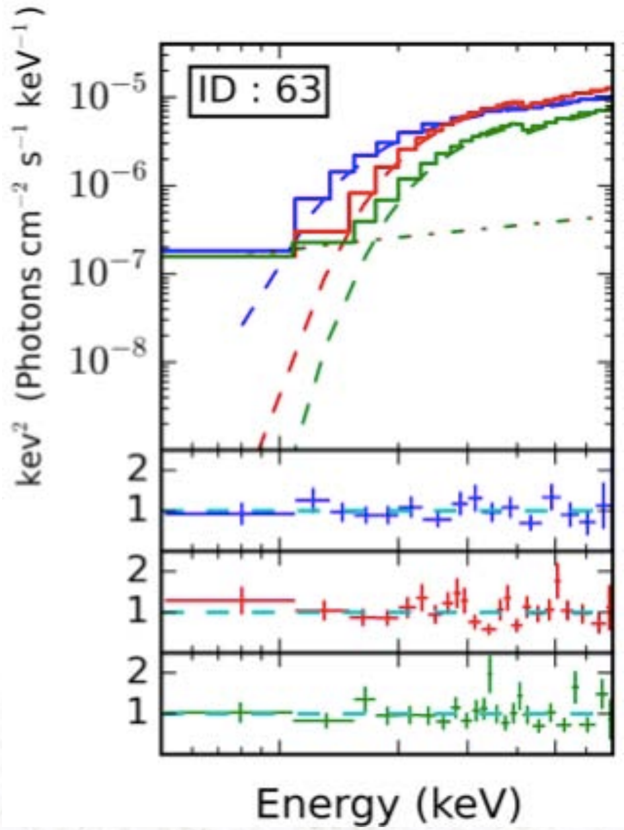

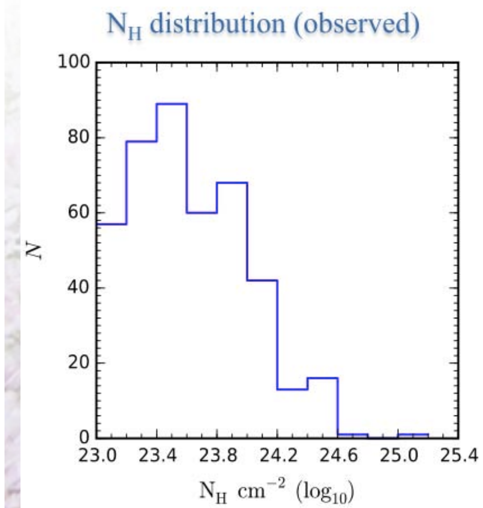

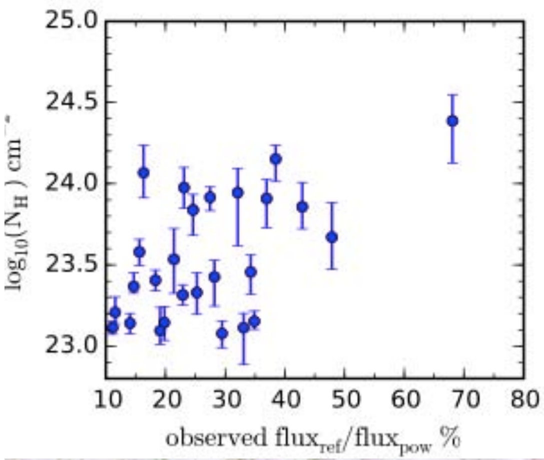

35% : N_H-variable 58% : L_X-variable

ID	d.o.f	model	L_X	$L_{X,AIC}$	$N_{H,AIC}$	$N_{H,exc}$	$error(N_{H,exc})$	f_{exc}	$error(f_{exc})$	pwl_{exc}	$error(pwl_{exc})$
73	3	A	3.410	4.560	0.690	-0.014	0.015	0.029	0.043	0.032	0.065
621	3	A	0.391	2.290	1.230	-0.009	0.010	-0.003	0.009	-0.007	0.012
846	3	A	0.837	0.150	1.150	-0.024	0.027	-0.010	0.010	-0.019	0.019
63	3	B	0.460	7.650	34.300	0.149	0.179	0.053	0.072	0.026	0.038
249	3	B	0.198	0.650	19.700	0.111	0.159	0.069	0.088	-0.048	0.073
785	3	B	6.292	7.670	0.210	-0.016	0.019	0.046	0.063	0.044	0.068
328	3	C	4.530	11.260	3.990	0.009	0.013	0.049	0.062	0.093	0.161
367	3	C	0.137	2.920	1.250	-0.014	0.021	0.044	0.056	0.041	0.056
399	3	C	0.371	12.240	2.650	-0.007	0.025	0.050	0.064	0.118	0.148

Great Future Field: Wide CDF-S Area

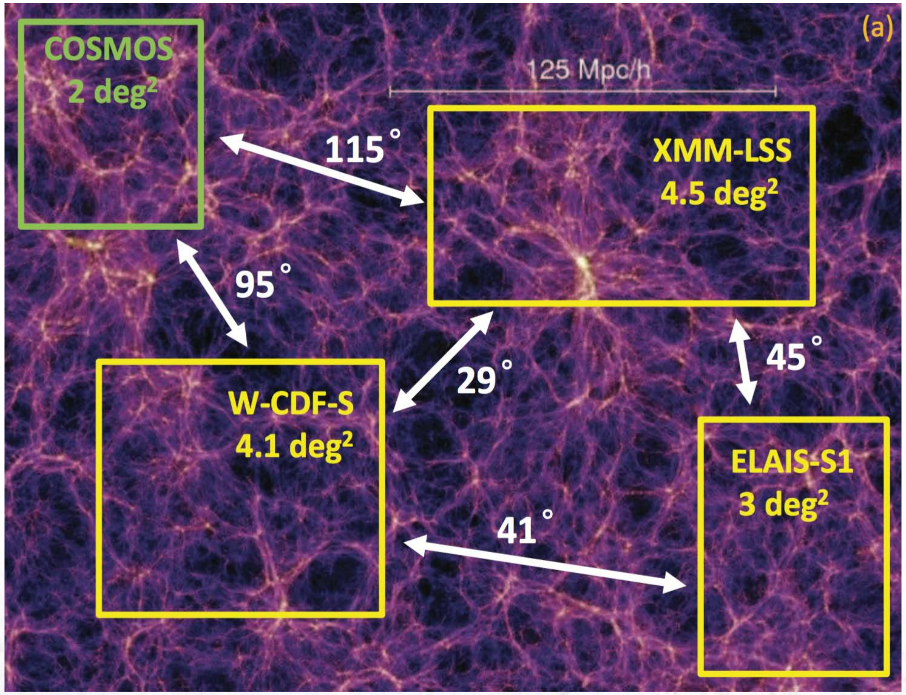

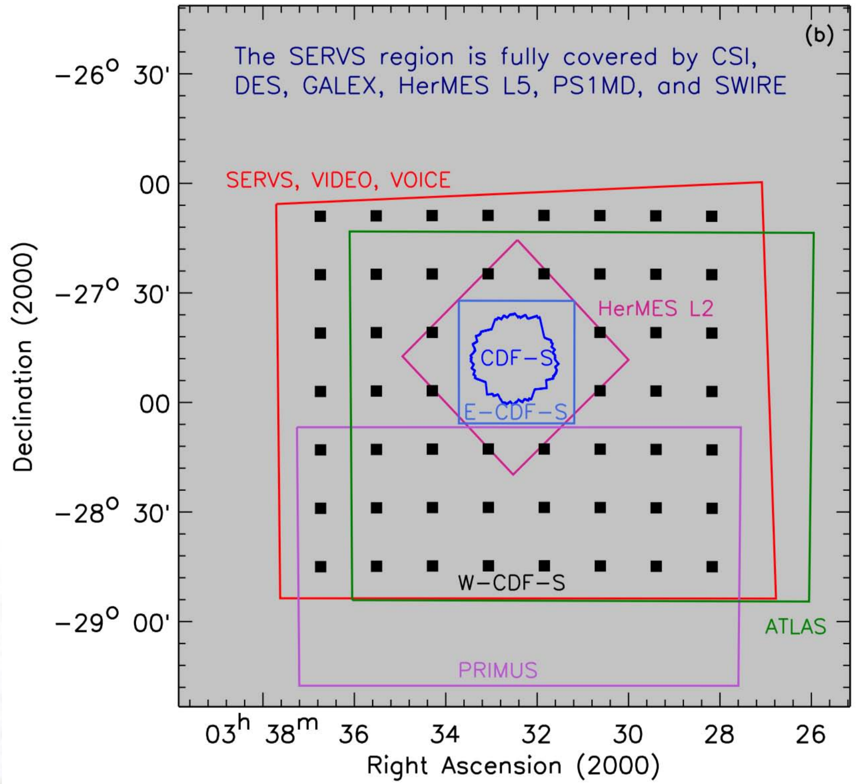

Study SMBH growth across the full range of cosmic environments – voids to massive clusters.

~5000 AGNs expected, for studies of AGNs and their connections to the host galaxies and environment.

Great Future Field: Wide CDF-S Area

Table 1: Current/Scheduled 1–10 deg^2 Multiwavelength Coverage of the W-CDF-S

Band	Survey Name and Solid-Angle Coverage	Comments
Radio	Australia Telescope Large Area Survey (**ATLAS**; 3.7 deg^2)[a]	15 μJy rms depth at 1.4 GHz
	MIGHTEE Survey (Scheduled; 4.5 deg^2)[b]	1 μJy rms depth at 1.4 GHz
FIR	*Herschel* Multi-tiered Extragal. Survey (**HerMES**; 0.6–11 deg^2)[c]	5–60 mJy depth at 100–500 μm
MIR	*Spitzer* Wide-area InfraRed Extragal. Survey (**SWIRE**; 6.6 deg^2)[d]	3.6–160 μm
NIR	*Spitzer* Extragal. Representative Volume Survey (**SERVS**; 4.5 deg^2)[e]	2 μJy depth at 3.6 and 4.5 μm
	VISTA Deep Extragal. Observations Survey (**VIDEO**; 4.5 deg^2)[f]	$ZYJHK_s$ to $m_{\rm AB} \approx 23.5$–25.7
Optical Photometry	Dark Energy Survey (**DES**; 9 deg^2 in 3 W-CDF-S fields)[g]	Multi-epoch *griz*; $m_{\rm AB} \approx 28$ co-added
	Pan-STARRS1 Medium-Deep Survey (**PS1MD**; 7 deg^2)[h]	Multi-epoch *grizy*; $m_{\rm AB} \approx 26$ co-added
	VST Optical Imaging of CDF-S and ES1 (**VOICE**; 4.5 deg^2)[i]	Multi-epoch *ugri*; $m_{\rm AB} \approx 26$ co-added
	SWIRE optical imaging (6.6 deg^2)[d]	
	LSST deep-drilling field (Planned; 10 deg^2)[j]	*ugrizy*; 20 000 visits total
Optical/NIR Spectroscopy	Carnegie-*Spitzer*-IMACS Survey (**CSI**; 6 deg^2)[k]	40 000 redshifts, 3.6 μm selected
	PRIsm MUlti-object Survey (**PRIMUS**; 1.95 deg^2)[l]	20 800 redshifts to $i_{\rm AB} \approx 23.5$
	VLT **MOONS** Survey (Scheduled; 4.5 deg^2)[m]	80 000 redshifts
	Spectroscopy of $\approx$ 900 radio and IR-luminous galaxies in ATLAS[n]	
UV	*GALEX* Deep Imaging Survey (7 deg^2)[o]	Depth $m_{\rm AB} \approx 25$

- LSST deep-drilling field: 5300-13800 visits per band (*ugrizy*) over ~ 10 year period.
- 4MOST (4-metre Multi-Object Spectroscopic Telescope)? MSE (Maunakea Spectroscopic Explorer)?

The end